THE OPTIMAL COASTAL RETRACKED SEA LEVELS FROM SARAL/ALTIKA SATELLITE ALTIMETRY OVER THE SOUTHEAST ASIA

NOOR NABILAH BINTI ABDULLAH

UNIVERSITI TEKNOLOGI MALAYSIA

THE OPTIMAL COASTAL RETRACKED SEA LEVELS FROM SARAL/ALTIKA SATELLITE ALTIMETRY OVER THE SOUTHEAST ASIA

NOOR NABILAH BINTI ABDULLAH

A report submitted in fulfilment of the
requirements for the award of the degree of
Master of Philosophy

Faculty of Geoinformation and Real Estate
Universiti Teknologi Malaysia

APRIL 2018

ACKNOWLEDGEMENTS

First and foremost, I would like to express my sincere gratitude to my supervisor Dr. Nurul Hazrina Idris and my co-supervisor Dr. Nurul Hawani Idris for the continues support of my Master study and related research, for their enormous guidance, patient, motivation and knowledge. Their doors were always open whenever I ran into a trouble spot or had questions about my research or writing. They always steered me in the right direction whenever they thought I needed it.

I would also like to thank Dr. Dudy Wijaya from Institute Teknologi Bandung, Indonesia and Dr. Angela Maharaj from the University of New South Wales, Australia for their insightful suggestions, invaluable guidance and encouragement during much of this research and for providing some references and useful discussion, which incited me to widen my research from various perspectives.

Special acknowledgment to my seniors, my colleagues and my best friends for their helping hand in cordial supports, valuable information and guidance, which help me in completing the task through various stages. Thank you for providing me assistance at various occasions without which this study would not be possible.

At this juncture, I feel deeply honoured in expressing my profound gratitude and deepest regards to my mum and dad for their loves, bless and constant support from time to time. This support shall carry me a long way in the journey of life on which I am about to embark upon. Thank you for being a constant source of inspiration during the preparation of this study. And to them, I dedicated this work.

ABSTRACT

The current demand for accurate coastal altimetry data, particularly for the sea level has increased since human activities have become increasingly concentrated along coastal areas. Over coastal region, particularly within 10 km from the coastline, the altimeter footprint is severely contaminated by land and rough coastal sea states. The contamination leads to the low quality observations, thus creating a significant gap in data availability over the coast. The aim of this study is to evaluate the quality of coastal retracked sea level data from AltiKa satellite altimetry over the Southeast Asia region. In this study, high resolution (40 Hz) sea levels derived from the advanced AltiKa satellite altimetry are validated over the Southeast Asia coastal regions. The parameter of sea level is derived based on three standard retracking algorithms which are MLE-4, Ice-1 and Ice-2. The assessments of quantity and quality of the retracked sea levels data are conducted to identify the optimum retracker over the study regions, which are Andaman Sea, Strait of Malacca, South China Sea, Gulf of Thailand and Sulu Sea. The quantitative analysis involves the comparison between AltiKa and Jason-2 waveforms, the computation of percentage of data availability, and the minimum distance of Sea Level Anomaly (SLA) to the coastline. The qualitative analysis involves the relative validation with geoid height and absolute validation with tide gauge. In general, AltiKa measurement can obtain as close as 1 km to the coastline with ≥85% data availability. The Ice-1 retracker has shown an excellent performance with percentage of data availability at ≥90% and minimum distance as close as 0.9 km to the coastline. In term of quality, Ice-1 retracker shows the highest improvement of percentage (IMP) values over Andaman Sea, Sulu Sea and Strait of Malacca with IMPs of 19%, 16% and 43%, respectively. The Ice-1 retracker also shows the highest temporal correlation (up to 0.95) and the lowest root mean square (RMS) error up to 8 cm over distance less than 10 km for those three regions. Contrary, over the South China Sea, Ice-2 retracker has better performance when compared to other retrackers with IMP values of 43%. Over distance less than 10 km to the shore, the temporal correlation and RMS error reach up to 0.88 and 7 cm respectively. Over the Gulf of Thailand, the optimum retracker cannot be concluded due to unavailable tide gauge data. The Ice-1 is the optimum retracker over three out of four regions. Therefore, it is used to study the seasonal variability of sea levels over the Southeast Asia. The seasonal variability shows that the mean amplitude is up to 25 cm during the Northeast Monsoon and decreased by 9 cm during the Southwest Monsoon and between 2 to 9 cm during inter-monsoon seasons. In conclusion, the research has significantly contributed in defining the quantity and quality of the AltiKa SLAs in the coastal region of Southeast Asia. The results from comprehensive validation obtained in this research present a significant improvement in identifying the reliability and applicability of the AltiKa datasets and retracking algorithms over the coastal area of the study region.

ABSTRAK

Permintaan semasa untuk data altimetri pesisir yang tepat, terutamanya untuk paras laut telah meningkat sejak aktiviti manusia menjadi semakin tertumpu di sepanjang kawasan pantai. Di kawasan persisir, terutamanya dalam lingkungan 10 km dari garis pantai, jejak altimeter dicemari dengan teruk oleh tanah dan keadaan laut yang bergelora. Pencemaran membawa kepada cerapan yang berkualiti rendah, sekali gus mewujudkan jurang yang ketara dalam ketersediaan data di pantai. Tujuan kajian ini adalah untuk menilai kualiti data paras laut pesisir dari satelit AltiKa di rantau Asia Tenggara. Dalam kajian ini, aras laut beresolusi tinggi (40 Hz) yang diterbitkan daripada satelit altimetri termaju AltiKa disahkan di kawasan pantai Asia Tenggara. Parameter aras laut diterbitkan berdasarkan kepada tiga algoritma penjejak piawai iaitu MLE-4, Ice-1 dan Ice-2. Penilaian kuantiti dan kualiti data aras laut yang telah menjalani pembetulan dijalankan untuk mengenal pasti penjejak yang optimum di kawasan kajian iaitu Laut Andaman, Selat Melaka, Laut China Selatan, Teluk Thailand dan Laut Sulu. Analisis kuantitatif melibatkan perbandingan antara bentuk gelombang AltiKa dan Jason-2, pengiraan peratusan ketersediaan data, dan jarak minimum aras anomali laut (SLA) ke garis pantai. Analisa kualitatif melibatkan pengesahan relatif dengan ketinggian geoid dan pengesahan mutlak dengan pengukur tolok pasang surut. Secara umumnya, pengukuran AltiKa dapat mencapai sehingga 1 km ke garis pantai dengan ketersediaan data ≥85%. Penjejak Ice-1 telah menunjukkan prestasi cemerlang dengan peratusan ketersediaan data pada ≥90% dan jarak minimum sehingga 0.9 km ke garis pantai. Dari segi kualiti data, penjejak Ice-1 menunjukkan nilai-nilai peratusan peningkatan (IMP) tertinggi di Laut Andaman, Laut Sulu dan Selat Melaka dengan IMP masing-masing sebanyak 19%, 16% dan 43%. Penjejak Ice-1 juga menunjukkan korelasi temporal tertinggi (sehingga 0.95) dan ralat punca kuasa min (RMS) yang terendah sehingga 8 cm pada jarak kurang daripada 10 km untuk ketiga-tiga kawasan tersebut. Sebaliknya, di Laut China Selatan, penjejak Ice-2 mempunyai prestasi yang lebih baik berbanding penjejak yang lain dengan nilai IMP 43%. Bagi jarak kurang daripada 10 km ke garis pantai, korelasi temporal dan ralat RMS masing-masing mencapai sehingga 0.88 dan 7 cm. Di Teluk Thailand, penjejak yang optimum tidak dapat disimpulkan disebabkan oleh ketiadaan data tolok pasang surut. Ice-1 adalah penjejak yang optimum di tiga daripada empat kawasan. Oleh itu, ianya digunakan untuk kajian variasi bermusim bagi aras laut di rantau Asia Tenggara. Variasi bermusim menunjukkan min amplitud adalah sehingga 25 cm semasa musim Monsun Timur Laut dan menurun sebanyak 9 cm semasa musim Monsun Barat Daya dan diantara 2 hingga 9 cm semasa musim peralihan monsoon. Kesimpulannya, penyelidikan ini telah menyumbang secara ketara dalam menentukan kuantiti dan kualiti data SLA AltiKa di rantau pantai Asia Tenggara. Hasil daripada pengesahan komprehensif yang diperolehi dalam kajian ini menunjukkan peningkatan yang ketara dalam mengenal pasti kebolehpercayaan dan kebolehgunaan data AltiKa dan algoritma penjejak di pesisir pantai dalam kawasan kajian.

TABLE OF CONTENTS

CHAPTER	TITLE	PAGE
	DECLARATION	**ii**
	ACKNOWLEDGEMENTS	**iii**
	ABSTRACT	**iv**
	ABSTRAK	**v**
	TABLE OF CONTENTS	**vi**
	LIST OF TABLES	**x**
	LIST OF FIGURES	**xii**
	LIST OF ABBREVIATIONS	**xviii**
	LIST OF SYMBOLS	**xxi**
	LIST OF APPENDICES	**xxv**
1	**INTRODUCTION**	**1**
	1.1 Background of the Study	1
	1.2 Issues with Coastal Altimetry Data for Mapping Sea Level	6
	1.3 Research Questions	11
	1.4 Aim and Objectives of the Study	12
	1.5 Research Scope	12
	1.6 Significance of the Study	14
	1.7 Thesis Outline	15
2	**SATELLITE ALTIMETER FOR OCEAN GEOPHYSICAL STUDIES**	**17**
	2.1 Introduction	17
	2.2 Derivation of Sea Level from Satellite Altimetry	17

2.3 Waveform Retracking Algorithms 21
2.3.1 The Brown Model 23
2.3.2 Maximum Likelihood Estimation-4 Retracking Method 26
2.3.3 Ice-1 Retracking Method 29
2.3.4 Ice-2 Retracking Method 31
2.4 Effort in Bringing Altimeter Data Closer to the Coast 34
2.5 Information about SARAL/AltiKa Satellite Altimetry Mission 42
2.5.1 Issue with Clouds and Precipitation Effect on SARAL/AltiKa Ka-band 43
2.6 Relative and Absolute Validation of Satellite Altimetry 46
2.7 Prior Study on Sea Level over Southeast Asia Region 48
2.8 Summary 51

3 STUDY AREA AND RESEARCH METHODOLOGY 53
3.1 Description of Study Area 53
3.2 Research Methodology 54
3.3 Phase I: Data Acquisition 57
3.4 Phase II: Data Pre-processing 58
3.5 Phase III: Data Processing 61
3.4.1 Altimeter Data Processing 62
3.4.2 Tide Gauge Data Processing 65
3.4.3 Wind and Sea Surface Current Data Processing 66
3.6 Phase IV: Data Analysis 67
3.5.1 Comparison between AltiKa and Jason-2 Waveforms 67
3.5.2 Percentage of Data Availability and Minimum Distance from Coastline 68
3.5.3 Relative Comparison of AltiKa SSHs with Geoid Height 68
3.5.4 Absolute Validation of AltiKa SLAs with In-situ Tide Gauge 69

3.5.5 Analysis of the Optimum Retracker 71
3.7 Phase V: Mapping Seasonal Sea Level Variability 72
3.8 Summary 72

4 QUANTITATIVE ANALYSIS OF SEA LEVEL DATA AVAILABILITY OVER THE COASTAL REGIONS 73
4.1 Introduction 73
4.2 The Comparison between AltiKa and Jason-2 Waveforms 74
4.3 Data Availability of SARAL/AltiKa retracked SLA over the Coastal Region 81
4.4 The Minimum Distance of the SARAL/AltiKa retracked SLAs to the Coastline 88
4.5 Summary 90

5 QUALITATIVE ANALYSIS OF RETRACKED SEA LEVEL OVER COASTAL REGIONS 92
5.1 Introduction 92
5.2 Relative Comparison of Retracked SSHs with Geoid Height 93
5.3 Absolute Validation of Retracked SLAs with Tide Gauge 97
5.3.1 Validation near the Bintulu Tide Gauge 98
5.3.2 Validation near the Geting Tide Gauge 102
5.3.3 Validation near the Vung Tau Tide Gauge 106
5.3.4 Validation near the Langkawi Tide Gauge 110
5.3.5 Validation near the Ko Taphao Noi Tide Gauge 114
5.3.6 Validation near the Lubang Tide Gauge 118
5.3.7 Factor that Influence the Precission and Accuracy of SARAL/AltiKa Sea Level 123
5.4 Summary 124

6 SEASONAL PATTERN OF SEA LEVEL OVER THE SOUTHEAST ASIA AND THE INFLUENCE OF UPWELLING FEATURE IN COASTAL AREA 126

6.1 Introduction 126

6.2 Seasonal Variability of SLA and their Relationship with Sea surface current and Wind Speed over Southeast Asia 128

6.2.1 Physical Characteristics of Wind, Sea Surface Current, and SLA, and their Connections during the Northeast Monsoon 131

6.2.2 Physical Characteristics of Wind, Sea Surface Current, and SLA, and their Connection during the Southwest Monsoon Season 134

6.2.3 Physical Characteristics of Wind, Sea Surface Current, and SLA, and their Connection during the Inter-monsoon Season 137

6.3 The Influence of Upwelling Feature to the Sea Level Variability over South China Sea 141

6.4 Summary 145

7 CONCLUSIONS AND RECOMMENDATIONS 147

7.1 Summary of the Research 147

7.2 Summary of Findings 148

7.2.1 The Quantitative and Qualitative Analysis of the AltiKa Retracked Sea Level 149

7.2.2 Spatial and Temporal Seasonal Variability of Sea Level 150

7.3 Recommendations for Future Work 152

REFERENCES 154

LIST OF TABLES

TABLE NO.	TITLE	PAGE
2.1	Summary of retracking method utilised in the study.	22
2.2	The summary of previous study in improving the accuracy of altimetry measurement over the coastal area.	40
3.1	List of tide gauge stations utilised in this study.	58
3.2	Defined threshold for editing AltiKa Ka-band data.	59
3.3	Summary of adopted models for deriving geophysical corrections in the AltiKa SGDR product (AVISO 2013).	63
4.1	Mean of signal-to-noise ratio of AltiKa and Jason-2 at cross-over points.	80
5.1	Example of STDs and IMPs of retrackers calculated from 19 cycles for several passes of SARAL/AltiKa	95
5.2	Information of tide gauge stations and the corresponding passes.	97
5.3	The mean temporal correlation and RMS error of MLE-4, Ice-1, and Ice-2 retracked SLAs along pass 808 with respect to the Bintulu tide gauge.	101
5.4	The mean temporal correlation and RMS error of the MLE-4, Ice-1, and Ice-2 retracked SLAs along pass 494 with respect to the Geting tide gauge	106

5.5	The mean temporal correlation and RMS error of the MLE-4, Ice-1, and Ice-2 retracked SLAs along pass 479 with respect to the Vung Tau tide gauge.	110
5.6	The mean temporal correlation and RMS error of the MLE-4, Ice-1, and Ice-2 retracked SLAs along pass 122 with respect to the Langkawi tide gauge.	113
5.7	The mean temporal correlation and RMS error of the MLE-4, Ice-1, and Ice-2 retracked SLAs along pass 479 with respect to the Ko Taphao Noi tide gauge.	118
5.8	The mean of temporal correlation and RMS error of the MLE-4, Ice-1 and Ice-2 retracked SLAs along pass 006, with respect to the Lubang tide gauge.	123
6.1	SLA variability showing the values of minimum, maximum and average (in unit cm) over the monsoon seasons.	130

LIST OF FIGURES

FIGURE NO	TITLE	PAGE
1.1	Schematic altimeter waveform with the geophysical parameters that correspond to different parts of the waveform over homogenous ocean surface (adapted from Idris, 2014).	2
1.2	(Top panel) Schematic representation of pulse-limited altimeter short pulse propagation from the altimeter to the sea surface in the case of an ocean-to-land transition. B is the bandwidth of the altimeter in unit of Hertz; c is the speed of light; *c/(2B)* is the altimeter sampling rate; H is the altimeter height; τ_1 and τ_2 are the epoch of the first and last measurement; and τ_0 is the epoch with respect to the nominal tracking position. (Lower panel) Top-down view of the pulse limited footprint corresponding to each waveform gate (adapted from Gommenginger *et al.,* 2011).	8
1.3	Shape of waveform when approaching the coastline. The waveform (in red) does not conform to the Brown model when it gets close to the coast due to land contamination (http://www.coastalt.eu/coastalt-short-web-summary, access on 10 March 2015).	9
2.1	The principle of radar altimetry for retrieving sea level parameter.	18
2.2	Schematic diagram of the OCOG method (adapted from Gommenginger, *et al.,* 2011).	30
2.3	Schematic diagram of the Ice-2 retracking method. The blue line represents the altimetric waveform and the yellow line represents the fitting function from Ice-2 retracking (adapted from Legresy, *et al.,* 2005).	32
2.4	Schematic design of Ice-2 retracking method. The altimeter waveform is divided into four estimation windows, which are thermal noise, leading edge, trailing edge-1, and trailing edge-2.	32

2.5	(a) AltiKa waveforms over Pass 121 Cycle 5 during rain events, (b) collocated rain rate, (c) mean normalized waveforms in nominal conditions (black line) and during rain events delineated by the red dotted rectangles in (a) (red line, adapted from Tournadre, *et al.,* 2015).	45
3.1	The region of study area. Red marks indicate the tide gauge stations and green lines indicate the AltiKa ground passes. The blue lines are the AltiKa ground passes used for validation purposes.	54
3.2	Flowchart of research methodology.	56
3.3	(a) Tide data condition with spikes (red box), data gap (green box), and reference change (black box). (b) Tide data after data pre-processing.	61
3.4	Examples of tide gauge original time series (blue), the tidal anomaly computed from harmonic analysis (green) and the de-tided sea level (red) will be used for comparison with the altimeter at (a) Langkawi and (b) Geting tide gauge stations.	66
3.5	Time series of tide gauges and AltiKa SLAs after removing the mean difference between both datasets. The time series is plotted based on the nearest AltiKa point of respective passes with the respective tide gauges.	70
4.1	(a) AltiKa and Jason-2 ground passes 006 cycle 2 (in red) and 203 cycle 176 (in blue), respectively, near North Kalimantan. (b) and (c) Waveforms spectra corresponding to (a), for AltiKa and Jason-2, respectively. Green, black and purple lines represent the distance of 2 km, 4 km and 6 km to the coastline, respectively. (d) and (e) Waveform shapes related to locations and colours in (a), for AltiKa and Jason-2, respectively	75
4.2	AltiKa and Jason-2 waveforms pattern at cross-over point. (a) The location of cross-over point between AltiKa pass 836 and Jason-2 pass 12 near Basilan, Philippines. (b-g) Waveform patterns of both satellites from different cycles.	76
4.3	AltiKa and Jason-2 waveforms pattern at cross-over point. (a) The location of cross-over point between AltiKa pass 322 and Jason-2 pass 242 near Batam, Singapore. (b-g) Waveform patterns of both satellites from different cycles.	77

4.4	AltiKa and Jason-2 waveforms pattern at cross-over point. (a) The location of cross-over point between AltiKa pass 264 and Jason-2 pass 38 near Miri, Malaysia. (b-g) Waveform patterns of both satellites from different cycles.	78
4.5	AltiKa and Jason-2 waveforms pattern at cross-over point. (a) The location of cross-over point between AltiKa pass 249 and Jason-2 pass 103 near Lord Loughborough Island, Myanmar. (b-g) Waveform patterns of both satellites from different cycles.	79
4.6	AltiKa and Jason-2 waveforms pattern at cross-over point. (a) The location of cross-over point between AltiKa pass 494 and Jason-2 pass 64 near Koh Rong Island, Cambodia. (b-g) Waveform patterns of both satellites from different cycles.	79
4.7	(a) The data availability (in unit %) for MLE-4 retracked SLAs over the Southeast Asia. Close up for (b) Andaman Sea, (c) Gulf of Thailand, (d) Strait of Malacca, (e) South China Sea, and (f) Sulu Sea. Figure b-f are plotted in a different scale.	82
4.8	(a) The data availability (in unit %) for Ice-1 retracked SLAs over the Southeast Asia. Close up for (b) Andaman Sea, (c) Gulf of Thailand, (d) Strait of Malacca, (e) South China Sea, and (f) Sulu Sea. Figure b-f are plotted in a different scale.	83
4.9	(a) The data availability (in unit %) for Ice-2 retracked SLAs over the Southeast Asia. Close up for (b) Andaman Sea, (c) Gulf of Thailand, (d) Strait of Malacca, (e) South China Sea, and (f) Sulu Sea. Figure b-f are plotted in a different scale.	84
4.10	The data availability (in unit %) for MLE-4 retracked SLAs. Close up for (a) near Riau archipelago and (b) over Philippines coastal water.	85
4.11	The data availability (in unit %) for Ice-1 retracked SLAs. Close up for (a) near Riau archipelago and (b) over Philippines coastal water.	85
4.12	The data availability (in unit %) for Ice-2 retracked SLAs. Close up for (a) near Riau archipelago and (b) over Philippines coastal water.	86
4.13	Mean percentage of AltiKa data availability over five experimental regions computed within 30 km of the coastline. It is computed from 18 passes for the Andaman	87

Sea and the Strait of Malacca, 16 passes for the Gulf of Thailand, 30 passes for the South China Sea, and 17 passes for the Sulu Sea.

4.14 Mean of minimum distance of AltiKa MLE-4, Ice-1, and Ice-2 retracked SLAs to the coastline for several passes over the South-East Asia coastal regions, computed from 19 cycles. 89

4.15 Mean of minimum distance of AltiKa for MLE-4, Ice-1 and Ice-2 retracked SLAs to the coastline over five experimental regions, computed from 19 cycles. 90

5.1 The mean IMP of Ice-1 and Ice-2 retrackers that are computed within 30 km from the coastline. It is computed from 18 passes for the Andaman Sea and Strait of Malacca, 16 passes for the Gulf of Thailand, 30 passes for the South China Sea, and 17 passes for the Sulu Sea. 96

5.2 a) AltiKa satellite pass 808 near Bintulu tide gauge station, and b) waveform power spectra along the pass for cycle 2. 98

5.3 SLA time series along pass 808 near Bintulu tide gauge station at different distances from the coastline. *r* represents the temporal correlation of the AltiKa retracked SLA with respect to the tide gauge. 99

5.4 Spatial plot of the temporal correlation (left) and the RMS error (right) of SLAs from different retracking methods along AltiKa pass 808 with respect to the Bintulu tide gauge. Distance to coastline is shown in black line labelled as 5 km, 10 km, 30 km, and 50 km. 100

5.5 a) AltiKa satellite pass 494 near Geting tide gauge station, and b) waveform power spectra along the pass for cycle 2. 103

5.6 SLA time series along pass 494 near the Geting tide gauge station at different distances from the coastline. *r* represents the temporal correlation of the AltiKa retracked SLA with respect to the tide gauge. 103

5.7 Spatial plot of the temporal correlation and the RMS error of SLAs from different retracking methods along AltiKa pass 494, with respect to the Geting tide gauge. Distance from the coastline is shown by the black line labelled as 5 km, 10 km, 30 km, and 50 km. 104

5.8	a) AltiKa satellite pass 479 near the Vung Tau tide gauge station, and b) waveform power spectra along the pass for cycle 2.	107
5.9	SLA time series along pass 479 near the Vung Tau tide gauge station at different distances to the coastline. *r* represents the temporal correlation of the AltiKa retracked SLA with respect to the tide gauge.	107
5.10	Spatial plot of the temporal correlation and the RMS error of SLAs from different retracking methods along AltiKa pass 479 with respect to the Vung Tau tide gauge. Distance to coastline is shown in black line labelled as 5 km, 10 km, 30 km, and 50 km.	109
5.11	a) AltiKa satellite pass 122 near the Langkawi tide gauge station, and b) waveform power spectra along the pass for cycle 2.	111
5.12	SLA time series along pass 122 near the Langkawi tide gauge station at different distances from the coastline. *r* represents the temporal correlation of the AltiKa retracked SLA with respect to the tide gauge.	111
5.13	Spatial plot of the temporal correlation and the RMS error of SLAs from different retracking methods along AltiKa pass 122, with respect to the Langkawi tide gauge. Distance to the coastline is shown in black line labelled as 5 km, 10 km, 30 km, and 50 km.	112
5.14	a) AltiKa satellite pass 537 near the Ko Taphao Noi tide gauge station, and b) waveform power spectra along the pass for cycle 2.	114
5.15	SLA time series along pass 537 near the Ko Taphao Noi tide gauge station at different distances from the coastline. *r* represents the temporal correlation of the AltiKa retracked SLA with respect to the tide gauge.	115
5.16	Spatial plot of the temporal correlation and the RMS error of SLAs from different retracking methods along AltiKa pass 537 with respect to the Ko Taphao Noi tide gauge. Distance from the coastline is shown in black line labelled as 5 km, 10 km, 30 km, and 50 km.	116
5.17	a) AltiKa satellite pass 006 near the Lubang tide gauge station, and b) waveform power spectra along the pass for cycle 2.	119
5.18	SLA time series along pass 006 near the Lubang tide gauge station at different distances from the coastline. *r*	119

represents the temporal correlation of the AltiKa retracked SLA with respect to the tide gauge.

5.19 Spatial plot of the temporal correlation and the RMS error of SLAs from different retracking methods along AltiKa pass 006, with respect to the Lubang tide gauge. Distance to the coastline is shown in black line labelled as 5 km, 10 km, 30 km, and 50 km. 122

6.1 Map of SLAs (in unit cm) during the Northeast Monsoon overlaid with: a) wind speed (in unit cm/s), and b) sea surface current (in unit cm/s). 133

6.2 The average sea surface current circulation adapted from Fang, *et al.,* (2009) during the Northeast Monsoon. 134

6.3 Map of SLAs (in unit cm) during the Southwest Monsoon overlaid with: a) wind speed (in unit cm/s), and b) sea surface current (in unit cm/s). 136

6.4 The average sea surface current circulation adapted from Fang, *et al.,* (2009) during the Northeast Monsoon. 137

6.5 Map of SLAs (in unit cm) during the inter-monsoon season (April-May) overlaid with: a) wind speed (in unit cm/s) and b) sea surface current (in unit cm/s). 139

6.6 Map of SLAs (in unit cm) during the inter-monsoon season (September-October) overlaid with: a) wind speed (in unit cm/s) and b) sea surface current (in unit cm/s). 140

6.7 Map of SLAs (in unit cm) over east coast of Peninsular Malaysia during a) June, b) July, c) August and d) September with wind speed (in unit cm/s). 142

6.8 Monthly-mean MODIS SST (in unit °C) of 2002-2012, overlaid with monthly-mean wind (arrow) from the European Center of Medium-Range Weather Forecasts (ECMWF; adapted from Mohd Akhir *et al.,* 2015) 143

6.9 Map of SLAs (in unit cm) over Vietnamese coast during a) June, b) July, c) August and d) September with wind speed (in unit cm/s). 144

LIST OF ABBREVIATIONS

ADCP	-	Acoustic Doppler Current Profiler
ALTICORE	-	Altimetry in Coastal Region
AVISO	-	Archiving, Validation and Interpretation of Satellite Oceanographic Data
CIOSS	-	Cooperative Institute for Oceanographic Satellite Studies
CLS	-	Collected Localisation Satellites
CNES	-	Centre National d'Etudes Spatiales
COASTALT	-	Coastal Altimetry Community
CTOH	-	Center for Topographic studies of the Ocean and Hydrosphere
DSMM	-	Department of Survey and Mapping Malaysia
DORIS	-	Doppler Orbitography and Radiopositioning Integrated by Satellite
ECMWF	-	European Center of Medium-Range Weather Forecasts
EGM2008	-	Earth Gravitational Model 2008
ESA	-	European Space Agencies
FES	-	Finite Element Solution
GECKO	-	Global Surface Current Data Product
GNSS	-	Global Navigation Satellite System
GODAE	-	Global Ocean Data Assimilation Experiment

GPS	-	Global Positioning System
GRACE	-	Gravity Recovery and Climate Experimental
HF	-	High Frequency
IGOS	-	Integrated Global Observing Strategy
ILWC	-	Integrated Liquid Water Content
IMA	-	Inter-monsoon April And May
IMP	-	Improvement of Percentage
IMS	-	Inter-monsoon September and October
ISRO	-	Indian Space Research Organization
ITCZ	-	Intertropical Convergence Zone
MLE	-	Maximum Likelihood Estimator
MODIS	-	Moderate Resolution Imaging Spectroradiometer
MP	-	Matching Pursuit
MSSH	-	Mean Sea Surface Height
NOAA	-	National Oceanic and Atmospheric Administration
OCOG	-	Offset Center of Gravity
OSTST	-	Ocean Surface Topography Science Team
PEACHI	-	Prototype for Expertise an AltiKa for Coastal, Hydrology and Ice
PISTACH	-	Coastal and Inland Water Innovative Altimetry Processing Prototype
PTR	-	Point Target Respond
RMS	-	Root Mean Square
SGDR	-	Sensor Geophysical Data Record

SIGDR	-	Sensor Interim Geophysical Data Record
SLA	-	Sea Level Anomaly
SNR	-	Signal-to-Noise Ratio
SPCZ	-	South Pacific Convergence Zone
SSB	-	Sea State Bias
SSH	-	Sea Surface Height
STD	-	Standard Deviation of Difference
SWH	-	Significant Wave Height
UHSLC	-	University of Hawaii Sea Level Centre
USO		Ultra-stable Oscillator
ZPD	-	Zenith Total Delay
ZWD	-	Zenith Wet Delay

LIST OF SYMBOLS

$R_{retracted}$	-	Range correction
R_{dry}	-	Dry tropospheric correction
R_{wet}	-	Wet tropospheric correction
R_{iono}	-	Ionospheric correction
$R_{corrected}$	-	Corrected range
R_{obs}	-	Observed range
t	-	Time
c	-	Speed of radar pulse
H	-	Satellite altitude
h	-	Height
h_{geoid}	-	Geoid height
h_{tides}	-	Tides
h_{atm}	-	Dynamic atmospheric correction
h_D	-	Sea surface height
h_{MSSH}	-	Mean sea surface height
h_{SLA}	-	Sea level anomaly
P	-	Satellite return power
P_{FS}	-	Flat surface response

P_{PT} - Theoretical point target response

q - Probability density function

B - Reception bandwidth of the altimeter

σ_p - Width of the radar point target response function

r_t - Time resolution

ξ - Off-nadir pointing angle

σ_s - Standard deviation of sea surface elevation

U - Unit step function

I_0 - Bessel function

A - Amplitude

G_0 - Radar system parameters of gain of the radar antenna

λ - Radar carrier wavelength

L_p - Two-way propagation loss

h_s - Modified satellite altitude

R_t - Radius of the Earth

γ - Antenna bandwidth

P_N - Altimeter's thermal noise

σ - Rise time

T - Units of satellite altimeter gates divided by sampling time

g_0 - Expected tracking gate in unit waveform gates

N - Number of pulses averaged

n - Number of bins or gates in each waveforms

$\hat{u}_i$	-	Measured return power
u_i	-	Theoretical return power
P_r	-	Return power of the surface
T_N	-	Denotes thermal noise
θ_j	-	Retrieved parameters
V	-	Variance-covariance matrix
F	-	Fisher information matrix
δ_{ir}	-	Kronecker delta (function of two variable of positive integers)
$n_{parameters}$	-	Number of parameters
W	-	Width of the waveform
COG	-	Waveform center of gravity
P_i	-	Waveform power
N_w	-	Total number of samples in the waveform
LEP	-	Leading edge position
m	-	Threshold value
G_r	-	Retracked range of the leading edge of the waveform
G_k	-	Power at the gate
k	-	Location of the first gate exceeding
S_t	-	Slope of the logarithm of the trailing edge
τ	-	Epoch
σ_L	-	Width of the leading edge
P_t	-	Mean power of the waveform

σ_c	-	Standard deviation of the ocean wave height
A_u	-	Amplitude of the waveform
V_h	-	Wind/current speed
u	-	Zonal component
v	-	Meridional component
ØVECT	-	Wind/current vector azimuth in unit degree
IMP	-	Improvement of percentage
σ_{MLE4}	-	Standard deviation of difference (STD) between MLE-4 retracked SSH and geoid heights
$\sigma_{retracked}$	-	STD of different between Ice-1 or Ice-2 retracked sea levels and geoid heights
r	-	Correlation
n	-	Number of pair data
x	-	Altimeter data
y	-	Tide gauge data

LIST OF APPENDICES

TABLE NO.	TITLE	PAGE
A	List of Publications	175

CHAPTER 1

INTRODUCTION

1.1 Background of the Study

Satellite altimeter is a nadir pointing microwave instrument that measures the distance between the satellite and the target surface. It is a matured discipline that provides accurate measurements of ocean geophysical information of significant wave heights (SWHs), sea surface height (SSHs), and wind speed over the open ocean (Gommenginger *et al.*, 2011). Satellite altimeter also one of the most important techniques for operational oceanography, particularly in providing a continuity of the data record (Le Traon *et al.*, 2015). Moreover, satellite altimeter can provide high quality data in global scale with a sufficiently dense space and time sampling (Le Traon, 2011; Le Traon *et al.*, 2015).

The concept of altimeter measurements is to measure two-ways travel time of pulse. The satellite altimeter emits pulses and analyses the returned signals reflected by the Earth's surface. Satellite position is referred to the ellipsoid (e.g., WGS84) and is precisely measured through orbit determination by using Doppler Orbitography and Radiopositioning Integrated by Satellite (DORIS), or Global Positioning System (GPS) receivers, or both (Benveniste, 2011).

Waveform is the altimetry radar-returned signal that represents the time evolution of the reflected power as the pulse hits the surface. Waveforms over the open ocean (without land contamination) can be described by Brown (1977) model (Figure

1.1). A Brown-like or ocean-like waveform features a leading edge which has a sharp rise up to a maximum value, followed by a trailing edge, which is a gently sloping plateau. The parameters of the mid-point of the leading edge are associated with altimeter range (referred to as epoch) which can be used to estimate the SSH. The slope of the leading edge is associated with the SWH. The wind speed can be derived from the amplitude of the waveform.

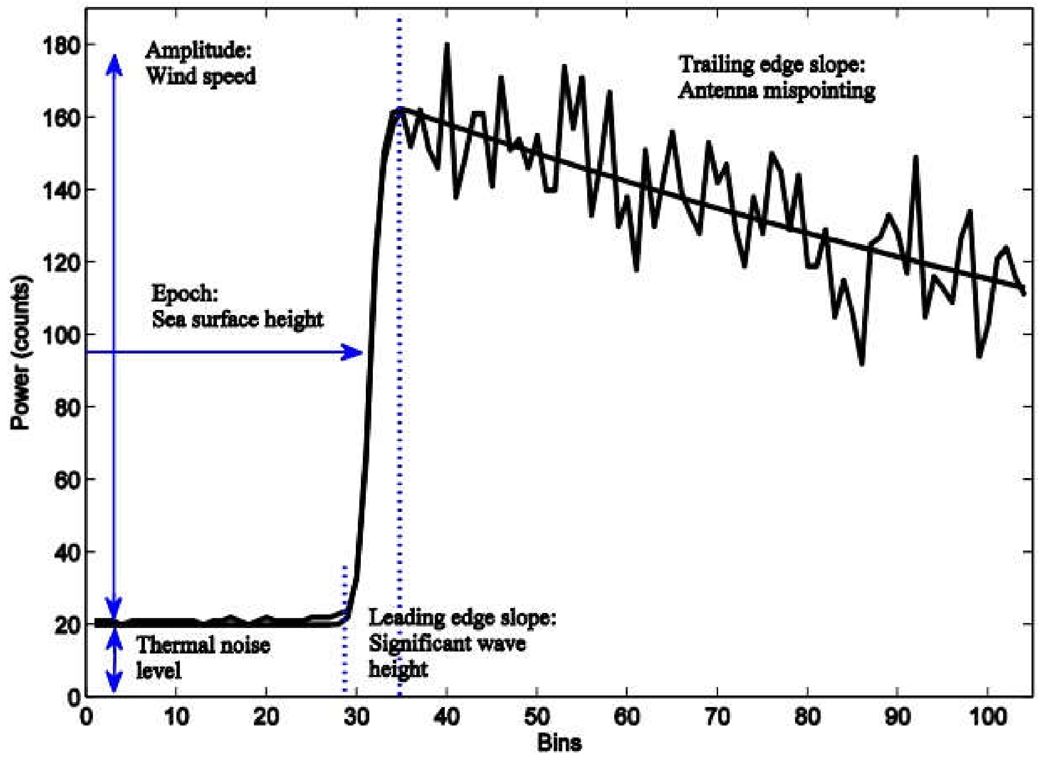

Figure 1.1: Schematic altimeter waveform with the geophysical parameters that correspond to different parts of the waveform over homogenous ocean surface (adapted from Idris, 2014).

Altimeter instruments can only measure returned signals in a narrow range window (typically 60 mm in vertical), called the 'analysis window'. In order to keep the reflected signals from the surface within the altimeter analysis window, an on-board tracker is used (Gommenginger *et al.*, 2011). Closed-loop regulators are used to measure the time delay between transmitted pulse and return pulse by using an α-β tracker and to keep the reflected signal within the altimeter analysis window (Gommenginger *et al.*, 2011). It holds the waveform's nominal position at a fixed point and amplitude with the intention of keeping the leading edge of the return pulse in the middle position of the sample at a corresponding time interval. The Maximum Likelihood Estimator (MLE) algorithm is applied to waveforms to fit the Brown (1977) model for retrieving ocean parameters (Idris, 2014). This is applied on-board the satellite. In order to gain the maximum accuracy of ocean parameters and to retrieve the final geophysical parameters, waveform retracking is performed on the ground. Waveform retracking is the procedure of post-processing to fit a functional form or model to the measured waveform. In order to improve parameter estimates (i.e., the power amplitude, epoch, and slopes of leading edge and trailing edge) over those estimated by the satellite on-board tracker, the retracking method is applied (Gommenginger *et al.*, 2011).

Over the last 30 years, numerous satellite altimeter missions have been launched such as Topex/Poseidon, ERS-1, ERS-2, Envisat, Jason-1, Jason-2, Jason-3, Cryosat-2, and the SARAL/AltiKa (hereafter referred as AltiKa). The Envisat and Jason-1 altimeter missions were officially retired in April 2012 and June 2013, respectively. In July 2008, Jason-2 was launched and flew on almost identical orbits with Jason-1, ~1 minute apart during the calibration phase (Idris, 2014). Then, in May 2012, the Jason-1 satellite was shifted to a lower orbit to begin its geodetic mission until it was decommissioned in July 2013. The Jason-3 was launched in February 2016 with a mission to extend the time series of ocean surface topography measurements of Topex/Poseidon, Jason-1, and Jason-2. The Cryosat-2 was launched in 2010 and equipped with an advanced microwave delay-Doppler/Synthetic Aperture Radar. It produces a footprint that is beam-limited in the along-track direction, which is in contract with the conventional ocean-viewing radar altimeter (such as Jason-1) that produces pulse limited footprint. The advancement in the accuracy, repeatability, and stability of satellite altimeters over the open ocean make them an irreplaceable tool for various ocean applications, including mapping ocean dynamics and circulations at high temporal and spatial scales..

However, in the vicinity of land near the coast, a number of issues arise when satellite altimetry attempts to monitor the sea level. The main issues are related to poorer geophysical corrections and artefacts in the altimeter return signals due to the existence of land within the altimeter footprint. In order to fulfil the increasing demand for satellite altimetry observation in coastal zones, where a diversity of human activities occur, the new generation of the AltiKa satellite altimetry mission was launched on 25th February 2013 by the Indian Space Research Organization (ISRO)/Centre National d'Etudes Spatiales (Vincent *et al.*, 2006; CNES,). The satellite mission provides opportunity from a space-borne Ka-band radar altimetry for nearly global (within +81.5º latitude bounds) synoptic mapping of ocean surfaces at monthly sampling (35-day repeat sun-synchronous orbit), and with higher spatial resolution (up to 40 Hz) than the present Ku-band (up to 20 Hz) altimetry such as Jason-1 and Jason-2. With the high rate along-track observations, the spatial resolution near the coast can be increased, thus enabling coastal observations much closer to the coast (Vincent *et al.*, 2006).

The large bandwidth (500 MHz) in Ka-Band provides a better vertical resolution (~0.3m) than in Ku-Band (~0.5 m, Vincent *et al.*, 2006). Moreover, the AltiKa satellite is equipped with a smaller antenna beam width (0.6°) than its successor mission of Envisat (1.29° for Ku-band and 5.5° for S band), thus producing a smaller size footprint (~4 km, Valladeau *et al.*, 2014). Smaller footprint size contributes to the improvement of the spatial resolution and segregating the type of surface in transition zones, such as coastal regions and sea ice boundaries. Nevertheless, Ka-band frequency is sensitive to atmospheric conditions, which may cause significant atmospheric attenuation (Vincent *et al.*, 2006). However, research by Tournadre *et al.* (2015) has found that the impact of atmospheric attenuation on the Ka-band signal on the AltiKa altimetry is not as severe as expected. When using a standard systematic flagging, 15% of data are flagged as bad. Of 15%, only 5.5% of data are affected by atmospheric attenuation.

In March 2015, there was a technical issue on the reaction wheels of AltiKa, which made it drift from the original orbit. Due to the situation, ISRO and CNES decided to pursue the mission with new phase called "SARAL-DP", an abbreviation for AltiKa – Drifting Phase. Starting from July 2016, the AltiKa satellite flies freely and repetitive ground passes are no longer maintained (Bron *et al.*, 2016). Since then, the AltiKa is referred to as a geodetic mission. The geodetic mission does not concern the repetitive orbit; the requirement of this mission is the high spatial resolution of data collection over at least 95% of all available ocean coverage (Bronner and Dibarboure, 2012). It means that AltiKa will continue to provide valuable data for mesoscale and operational geography.

The Prototype for Expertise, an AltiKa for Coastal, Hydrology and Ice (PEACHI) project, is specifically conducted for the AltiKa mission. The aim is to perform a new retracking algorithm for the 40 Hz AltiKa data in order to improve the accuracy of estimates for scientific applications, such as coastal area, surface hydrology, ice, and open ocean (Poisson *et al.*, 2013; Valladeau *et al.*, 2014; Valladeau *et al.*, 2015). The project utilised along-track Sensor Geophysical Data Record (SGDR) and Sensor Interim Geophysical Data Record (SIGDR) in its processing scheme.

The standard retracking algorithms used in SGDR and SIGDR data products are MLE-4, Ice-1 and Ice-2. The MLE-4 algorithm includes the second order Bessel function of the Brown (1977) model to account for the antenna mispointing angle (Amarouche *et al.*, 2004; Thibaut *et al.*, 2010). It estimates four parameters which are the range, slope of leading edge, power amplitude, and antenna off-nadir angle by fitting the model to the waveform. It is also capable of improving the range and slope of leading edge estimates, especially when the return pulses do not fully conform to the Brown model (Thibaut *et al.*, 2010). This contributes to improving the accuracy and allows for measurements closer to the coastline. The Ice retrackers are based on the statistics of the waveform shapes. It estimates two parameters, which are power amplitude and range (Idris and Deng, 2012). More information about retracking algorithms is discussed in Chapter 2.

This research has been conducted to provide necessary steps in defining the quantity and quality of AltiKa sea level in coastal region of Southeast Asia. It is to identify the reliability and capability of AltiKa datasets and find the optimal retracking algorithms over the coastal area of study region.

1.2 Issues with Coastal Altimetry Data for Mapping Sea Level

Conventional satellite altimetry (e.g. Jason-1, Jason-2 and ENVISAT) can provide highly accurate sea level measurement (in cm level) over the open ocean due to proper modelling of ocean state qualities (e.g. tides) and accurate measurement of atmospheric refractions (Bouffard *et al.*, 2008). The satellite altimetry is capable of providing accurate information of ocean properties that can achieve an accuracy of up to 4 cm in height measurements (Challenor *et al.*, 1996; Fu and Cazenave, 2001) and 2-3 cm in mean sea level variations (Gómez-Enri *et al.*, 2008). However, in coastal regions, altimetry and its applications still face many challenges (e.g. Anzenhofer *et al.*, 1999; Bouffard *et al.*, 2010; Gommenginger *et al.*, 2011; Vignudelli *et al.*, 2011; Cipollini, 2013). The accuracy of sea level measurements decreases abruptly as the altimeter approaches the coast, where the sea conditions can diverge drastically over time and space.

An accurate sea level observation over the coastal region has been in great demand by the local scientific community for various applications. The desired accuracy of derived geophysical information varies depending on the applications. For example, the accuracy desired for measuring sea level rise is 1 mm/year and a 10 cm accuracy is required for detecting eddies in the East Australian Current system (Idris, 2014). The accuracy desired for measuring sea level rise is 1 mm/year over Malaysia seas (Md Din, 2010) and a 7.5 cm accuracy is required for detecting eddies in the South China Sea (Yi *et al.*, 2014). With the current altimeter, the accuracy of sea level in the open ocean is at 2-3 cm. However, this value is higher towards the coast (Andersen and Scharroo, 2011).

Two major challenges of using satellite altimetry for monitoring the sea level in coastal regions (i.e. less than 10 km from the coastline) are: 1) waveform distortion due to non-ocean like reflection (land contamination), and 2) geophysical corrections for retrieving sea level.

The distortion of altimetric waveforms occurs due to the land contamination within the altimeter footprint and rapid changes in sea state. The altimetry data become unreliable as the sea floor topography becomes shallow abruptly and there are major surface changes rapidly between land and ocean (Brooks *et al.*, 1998; Le Traon and Morrow, 2001; Deng *et al.*, 2002; Idris and Deng, 2012). With the previous generation of radar altimeters (i.e., Jason-1, Jason-2 and Envisat), the coastal water is poorly observed within ~15 km of the shoreline (Deng *et al.*, 2002; Idris and Deng, 2012) around the Australian coastal water, and within ~10 km around the South China Sea coastal water (Kuo *et al.*, 2012).

When an altimeter encounters the transition zone (land-to-ocean or ocean-to-land), the altimeter footprint is partly over ocean and partly over land, making more waveform samples contaminated by non-ocean like reflection, as shown in Figure 1.2. The power received at a given gate is correlated with the relative fraction of sea and land areas in the corresponding footprint and with the reflective properties of each type of surface (Gommenginger *et al.*, 2011). The lower panel of Figure 1.2 indicates the top-down view of the pulse-limited footprint corresponding to each waveform gate. It shows the relative proportion of ocean and land part in each of annuli away from the nadir point.

As the satellite approaches the coast, the altimeter waveform does not conform to the Brown model, and thus the general satellite on-board tracker system fails to precisely retrieve the geophysical parameters (Figure 1.3). As waveform samples are contaminated by non-ocean-like reflections, the high peaks show on the trailing edge (Gommenginger *et al.*, 2011). This issue leads to erroneous estimates of the geophysical information, thus resulting in systematic flagging and rejection of altimetric data and leave a ‘data gap’ in the coastal zone (Idris, 2014).

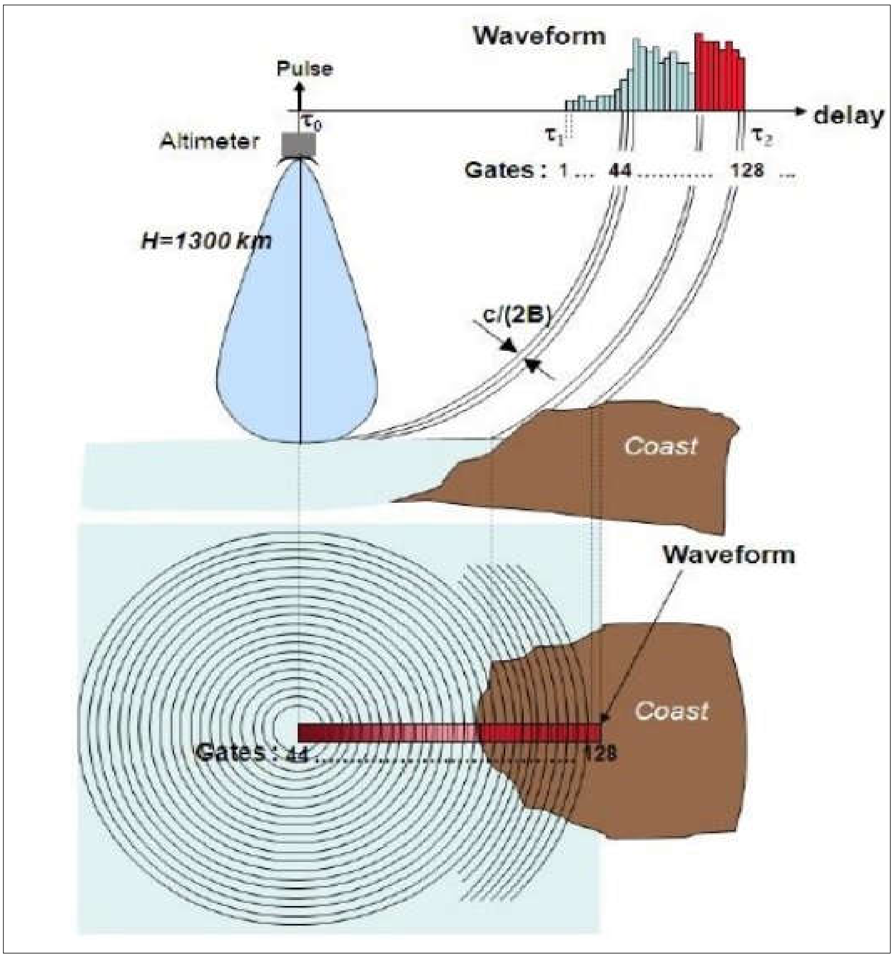

Figure 1.2: (Top panel) Schematic representation of pulse-limited altimeter short pulse propagation from the altimeter to the sea surface in the case of an ocean-to-land transition. B is the bandwidth of the altimeter in unit of Hertz; c is the speed of light; c/(2B) is the altimeter sampling rate; H is the altimeter height; τ_1 and τ_2 are the epoch of the first and last measurement; and τ_0 is the epoch with respect to the nominal tracking position. (Lower panel) Top-down view of the pulse limited footprint corresponding to each waveform gate (adapted from Gommenginger *et al.,* 2011).

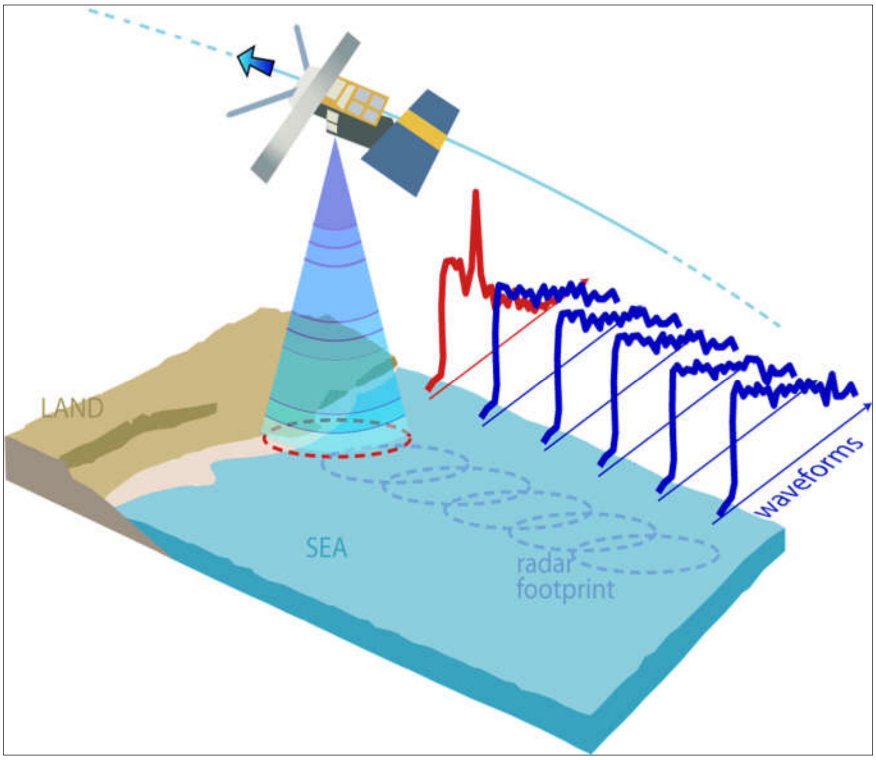

Figure 1.3: Shape of waveform when approaching the coastline. The waveform (in red) does not conform to the Brown model when it gets close to the coast due to land contamination (adapted from COASTALT, 2015).

The retrieval of sea level from the altimeter measurement involves a number of corrections for geophysical signals and atmospheric attenuations. The geophysical corrections (e.g., tides and atmospheric corrections) and environmental corrections (e.g., sea state bias, ionospheric, dry and wet tropospherics) become less reliable as the altimeter approaches the coastline (Andersen and Scharroo, 2011). These contribute to the degradation of accuracy in SSH measurements.

The wet tropospheric refraction is the major source of error in altimeter-derived sea level anomalies (SLAs) near the coast. This is because over the coastal region (~50 km from the coastline) the emissivity of land is much higher than the ocean and the presence of warm land corrupts the humidity retrieval methods. This consequently degrades the accuracy of the correction (cf. Andersen and Scharroo, 2011). For handling this issue, two strategies have been proposed. The first consists of merging the data in the coastal zones to update and improve the radiometer-derived wet tropospheric correction in the coastal area, and the second consists of the correction of the measured brightness temperatures for removing the contamination from the surrounding land (Obligis *et al.*, 2011). Further explanations and the outcomes about those approaches can be found in the book Coastal Altimetry by Vignudelli *et al.,* (2011), and in particular in the Chapter by Obligis *et al.,* (2011).

Another altimetric correction that presents the most significant challenge over the coastal region is sea state bias (SSB) correction. The SSB error is due to the bias of altimeter range measurement toward the trough of ocean waves (Gommenginger and Srokosz, 2006; Andersen and Scharroo, 2011). The SSB correction is inferred empirically, based on the wind speed and the SWH is derived from the waveform shape itself (AVISO, 2009). The complication of determining SSB correction near the coast is due to the wind propagation and the changing shape of the ocean waves, along with the interaction between bathymetry and coastal topography. This condition creates noisy waveforms and SWH accordingly.

Tidal variation is also one of the most significant error sources over the coastal region. Large error (>10-20 cm) in tidal models and the model utilised to approximate the inverse barometer correction remain a challenge in this area. There are two tidal models that are currently available in the SGDR product: the 2D Finite Element Solution (FES2012) and the Ocean Tidal Model (GOT4.8). The FES2012 is an improvement of FES2004. It is based on an assimilation of satellite altimetry into a time-stepping finite element hydrodynamic model (Lyard *et al.*, 2006; Carrère *et al.*, 2012). The GOT4.8 is based on the sequence of empirical ocean tide models derived from altimeter data (Ray, 2008). Previous research suggests that the FES tidal model is the best model for the marginal sea area (e.g. Md Din, 2010; Md Din and Omar, 2012; Md Din *et al.*, 2012; Md Din, 2014, Md Din, 2014).

There is also an issue with altimetric signal attenuation due to liquid water, such as rains and clouds. Due to wind and air flow, the distribution of rain is much higher over the coast than the open ocean. Radar altimetry signal can be strongly attenuated by light rain and small clouds, thus distorting the altimeter waveform (Tournadre, 1999). This can have a significant impact on geophysical parameter estimations and can cause 10-80% data loss (Tournadre *et al.*, 2009).

Due to the low quality of altimeter geophysical retrieval, coastal data are usually systematically flagged and rejected. This makes the coastal water poorly observed, particularly within ~15 km of the shoreline (Deng *et al.*, 2002; Idris and Deng, 2012). This flagged data, however, can be potentially recovered through the retracking method, and applying the newly developed geophysical corrections and processing schemes (e.g. Amarouche *et al.*, 2004; Vignudelli *et al.*, 2005; Lebedev *et al.*, 2008; Bao *et al.*, 2009; Idris and Deng, 2012; Idris, 2014) that optimise the estimation of geophysical parameters from the waveform on the ground processing. Retracking algorithms are developed to reprocess the original altimeter return signal by correcting the bias in estimation of geophysical parameters due to corrupted signals. A detailed explanation about the retracking algorithms is provided in Section 2.4.

The high rate along-track measurement of SSH offered by the AltiKa satellite altimetry mission should benefit the studies for understanding the sea level and its mesoscale variability. Thus, the exploitation of the AltiKa altimetry is needed for accurate mapping of coastal sea levels. This research is conducted to identify how much closer the retracked AltiKa sea level measurement can get to the coastline over the region of marginal seas in Southeast Asia, as well as to evaluate the precision and accuracy of the retracked sea levels over the experimental regions.

1.3 Research Questions

The research questions of the study are:

i. How much AltiKa sea level data can be recovered through the standard retracking algorithms?
ii. How much closer can the retracked sea level derived from the AltiKa Ka-band get to the coastline over the marginal seas of the Southeast Asia coastal region?
iii. How accurate is the retracked sea level from the AltiKa Ka-band satellite altimetry in the coastal region of Southeast Asia?

1.4 Aim and Objectives of the Study

The research aim is to evaluate the quality of coastal retracked sea level from SARAL/AltiKa satellite altimetry over the Southeast Asia region. The aim is accomplished through three (3) specific objectives:

i. To derive accurate SLAs from the AltiKa Ka-band based on three retracking algorithms of MLE-4, Ice-1 and Ice-2 in the SGDR data product;
ii. To assess the quantity and quality of retracked SLAs in identifying the optimum retracker for the marginal seas of Southeast Asia;
iii. To analyse the seasonal variability of SLA in Southeast Asia from the optimum retracked SLA in (ii).

1.5 Research Scope

In this research, the 40 Hz waveforms of the AltiKa satellite altimetry from cycles 1–19 (April 2013–December 2014) are utilised. It is realised that the altimetry data utilised in this study is in a short period. This is because, by the time this research started, only 19 cycle of AltiKa data are available. The study aims to derive a high resolution of sea levels above a reference ellipsoid from the SGDR retracked AltiKa data over the Southeast Asia region. The MLE-4, Ice-1, and Ice-2 retracking techniques are involved in the processing to derive sea level above a reference ellipsoid. These techniques should improve the accuracy of altimetry data sea levels near the coastal water.

The quantity of AltiKa data over the coastal region is assessed by comparing the AltiKa waveform and Jason-2 waveform at near parallel passes and crossover point, computing the percentage of data availability and the minimum distance of retracked sea level based of the number of valid datasets. This assessment can determine the capability of AltiKa in measuring the oceanic mesoscale variability over the coastal region. This also can determine how much data can be recovered through those three retracking algorithms (i.e. MLE-4, Ice-1, and Ice-2), and how much closer the AltiKa retracked data can get to the coastline compared to Jason-2.

The quality of the AltiKa retracked sea level is assessed by comparing the retracked sea level with quasi-independent and independent data. The assessments involved are: 1) a relative validation of retracked sea level with geoid height, and 2) an absolute validation of retracked sea level with independent tide gauge data.

The first assessment is to compare the retracked sea level from the retracking algorithms (i.e., MLE-4, Ice-1 and Ice-2) with the geoid height based on the Earth Gravitational Model (EGM2008). The precision of the sea level is assessed based on the standard deviation of difference between the retracked sea level and the geoid, and also the improvement of percentage (IMP). The second assessment is to compare the retracked sea levels with in-situ tide gauge data. The precision between altimetric and in-situ sea level measurement is determined by assessing the value of correlation coefficient, and the accuracy of the altimeter sea level is determined by assessing the root mean square error. These assessments are conducted to identify the reliability and accuracy of the retracked datasets, and to determine which retracker is the optimum for the study regions.

The derived sea level from the optimum retracker are mapped to analyse the seasonal variability of the sea level. This is to understand the spatial and temporal variability of sea level and to investigate the impact of Southwest monsoons and Northeast monsoons on the amplitude of the sea level over the region.

1.6 Significance of the Study

Nowadays, demand for accurate altimetry data over the coastal area, particularly the sea level, has risen since human activities are concentrated over this region. The increasing demand for coastal altimetry encompasses a wide range of applications such as hydrology, coastal erosion, cryosphere application, and flood risk appraisal. This results in much innovative research for improving coastal altimetry data. The no-data gap in coastal regions have been reduced from ~50 km to ~10 km from the coastline through various research in the last few years (e.g., Brooks *et al.,* 1997; Amarouche *et al.,* 2004; Deng and Featherstone, 2006; Idris and Deng, 2012, Babu *et al.*, 2015; Birol and Niño, 2015; Abdullah *et al.*, 2016). Nonetheless, the improvement of altimetry data is still challenging within ~10 km from the coastline (Idris, 2014), which is linked to the condition of land topography, rough/calm coastal sea state, and land contamination within the altimetry footprint. Therefore, this research provides a necessary step to derive accurate SLAs from AltiKa satellite altimetry. The framework developed in this research should enable the derivation of accurate sea levels over the Southeast Asia regions.

Moreover, much information can be retrieved by bringing the altimetry data closer to the coastline, exclusively in environmental sustainability for coastal management. Since human activities are primarily concentrated in coastal areas, studies about sea levels using satellite altimetry would give advantages, especially in engineering activities along the shoreline, and will hopefully benefit economic and recreational activities.

The launch of the AltiKa satellite mission promises a significant refinement of coastal altimetry, with advanced instruments, an improved retracking algorithm, and geophysical corrections (Cipollini, 2013; Prandi *et al.*, 2015; Ratheesh *et al.*, 2015; Schwatke *et al.*, 2015; Verron *et al.*, 2015). The validation and calibration for the satellite mission are compulsory to find the level of confidence on the data quality before it can be used in any applications. Global calibrations for AltiKa have been conducted by CNES, ISRO, and many other researchers (e.g., Gómez-Enri *et al.*, 2008; Abdalla, 2015; Prandi *et al.*, 2015; Tournadre *et al.*, 2015; Verron *et al.*, 2015). However, limited research focuses on the regional validation over Southeast Asia (e.g. Idris *et al.*, 2014b; Idris *et al.*, 2014c; Abdalla, 2015; Abdullah *et al.*, 2015; Mohammed *et al.*, 2015). The regional validation is important because the ocean characteristics of the region are significantly different than the other oceans, such as the Pacific and Atlantic Ocean. It is characterized by marginal and semi-closed oceans that contain many small islands and a broad range of topographic features, thus producing complicated waveform patterns when they enter the altimeter footprints. Therefore, this research is conducted to quantify the quality of sea levels derived from the AltiKa over the Southeast Asia region.

1.7 Thesis Outline

The thesis consists of seven chapters. Chapter 1 introduces the background of the research. Current issues associated with coastal altimetry are discussed and the objectives of the research are addressed. This study is mainly established for the marginal seas of Southeast Asia. Five seas are involved, including the Andaman Sea, the Gulf of Thailand, the Strait of Malacca, the South China Sea, and the Sulu Sea. This study is applied to the five different seas to identify its performance and applicability in different coastal regions.

Chapter 2 discusses the issues of satellite altimetry for ocean geophysical studies. The derivation of sea level from altimetry and the retracking algorithms utilised in this study are reviewed and discussed. The chapter also discusses the recent research conducted by international organisations and researchers in bringing altimeter measurements closer to the coastline.

Chapter 3 describes the research framework and methodology. The details about data pre-processing, data processing, derivation of sea level from the AltiKa satellite, and tide gauge measurements are provided in this chapter. The validation protocol and SLAs mapping are also described in detail.

In Chapter 4, the quantity of the AltiKa ret-racked sea level over the five regions is evaluated. The evaluation is based on:

i. The comparison of AltiKa Ka-band waveform patterns and Jason-2 Ku-band over the coastal area. Through this comparison, the impact of land contamination in coastal zones on both satellite returned signals can be

REFERENCES

Abdalla, S. (2014). Calibration of SARAL/AltiKa Wind Speed *IEEE Geoscience Remote Sensing Letters.* 11 1121 - 23.

Abdalla, S. (2015). SARAL/AltiKa Wind and Wave Products: Monitoring, Validation and Assimilation. *Marine Geodesy.* 38 (sup1), 365-80.

Abdullah, N. N., Idris, N. H. and Idris, N. H. (2015). Performance of SARAL/Altika Satellite Altimetry Mission over the Straits Of Malacca and the South China Sea. *IEEE Workshop on Geoscience and Remote Sensing 2015.* 16-17 November 2015. Kuala Lumpur, Malaysia, 86-89.

Abdullah, N. N., Idris, N. H. and Maharaj, A. M. (2016). The Retracked Sea Levels from SARAL/AltiKa Satellite Altimetry: The Case Study around the Strait of Malacca and the South China Sea. *International Journal of Geoinformatics.* 12 (2), 33-39.

Alvarez, R. A. (2016). *Hurricane Mitigation for the Built Environment.* New York: Taylor & Francis.

Amarouche, L., Thibaut, P., Zanife, O. Z., Dumont, J. P., Vincent, P. and Steunou, N. (2004). Improving the Jason-1 Ground Retracking to Better Account for Attitude Effects. *Marine Geodesy.* 27 (1-2), 171-97.

Amiruddin, A., Haigh, I., Tsimplis, M., Calafat, F. and Dangendorf, S. (2015). The Seasonal Cycle and Variability of Sea Level in The South China Sea. *Journal of Geophysical Research: Oceans.* 120 (8), 5490-513.

Andersen, O. B. (1995). Global Ocean Tides from ERS 1 and TOPEX/POSEIDON Altimetry. *Journal of Geophysical Research: Oceans.* 100 (C12), 25249-59.

Andersen, O. B. and Scharroo, R. (2011). Range and Geophysical Corrections in Coastal Regions: And Impications for Mean Surface Determination. In Vignudelli, S., Kostianoy, A. G., Cipollini, P. and Benveniste, J. *Coastal Altimetry.* (103-46). London, New York: Springer.

Anzenhofer, M., Shum, C. K. and Rentsh, M. (1999). *Coastal Altimetry and Application.* (1). Columbus, Ohio: Department of Civil and Environmental Engineering and Geodetic Science.

Apel, J. R., Holbrook, J. R., Liu, A. K. and Tsai, J. J. (1985). The Sulu Sea internal soliton experiment. *Journal of Physical Oceanography.* 15 (12), 1625-51.

AVISO (2008). Aviso and Podaac user handbook: IGDR and GDR Jason products. Available at: http://www.aviso.oceanobs.com/fileadmin/documents/data/tools/hdbk_j1_gdr.pdf

AVISO (2010). Coastal and Hydrology Altimetry Product Handbook. Available at: http://www.aviso.oceanobs.com/fileadmin/documents/data/tools/hdbk_Pistach.pdf

AVISO (2009). OSTM/Jason-2 Products Handbook. Available at: http://www.osdpd.noaa.gov/ml/ocean/J2_handbook_v1-4_no_rev.pdf

AVISO (2012). Validation of Altimeter Data by Comparison with Tide Gauges Measurements: 2012 Annual Validation Report. Available at: http://www.aviso.oceanobs.com/fileadmin/documents/calval/validation_report/insitu/annual_report_insitu_TG_2012.pdf

Babu, K., Shukla, A., Suchandra, A., Arun Kumar, S., Bonnefond, P., Testut, L., Mehra, P. and Laurain, O. (2015). Absolute Calibration of SARAL/AltiKa in Kavaratti during its Initial Calibration-VSalidation Phase. *Marine Geodesy.* 38 (sup1), 156-70.

Bao, L., Lu, Y. and Wang, Y. (2009). Improved Retracking Algorithm for Oceanic Altimeter Waveforms. *Progress in Natural Science.* 19 (2), 195-203.

Benveniste, J. (2011). Radar Altilmetry: Past, Present and Future. In Vignudelli, S., Kostianoy, A. G., Cipollini, P. and Benveniste, J. *Coastal Altimetry.* (1-18). London, New York: Springer.

Bertiger, W., Desai, S., Dorsey, A., Haines, B., Harvey, N., Kuang, D., Lane, C., Weis, J. and Sibores, A. (2008). Jason-2 Precision Orbit Determination Status. *OSTST Workshop.* Nov 2008. Nice,

Bessero, G. (1985). Marées, Service Hydrographique et Océanographique de la Marine. *Brest, France.*

Bhowmick, S. A., Modi, R., Sandhya, K., Seemanth, M., Balakrishnan Nair, T., Kumar, R. and Sharma, R. (2015a). Analysis of SARAL/AltiKa wind and wave over Indian Ocean and its real-time application in wave forecasting system at ISRO. *Marine Geodesy.* 38 (sup1), 396-408.

Bhowmick, S. A., Sharma, R., Babu, K., Shukla, A., Kumar, R., Venkatesan, R., Gairola, R., Bonnefond, P. and Picot, N. (2015b). Validation of SWH and SSHA from SARAL/AltiKa Using Jason-2 and In-Situ Observations. *Marine Geodesy.* 38 (sup1), 193-205.

Birol, F. and Niño, F. (2015). Ku and Ka-band Altimeter Data in the Northwestern Mediterranean Sea: Impact on the Observation of the Coastal Ocean Variability. *Marine Geodesy.* 38 (sup1), 313-27.

Bonnefond, P., Exertier, P., Laurain, O., Ménard, Y., Orsoni, A., Jeansou, E., Haines, B. J., Kubitschek, D. G. and Born, G. (2003). Leveling the sea surface using a GPS-catamaran special issue: Jason-1 calibration/validation. *Marine Geodesy.* 26 (3-4), 319-34.

Bonnefond, P., Haines, B. and Watson, C. (2011). In-situ Absolute Calibration and Validation: A Link from Coastal to Open Ocean Altimetry. In Vignudelli, S., Kostianoy, A. G., Cipollini, P. and Benveniste, J. *Coastal Altimetry.* (259-96). London, New York: Springer.

Born, G. H., Parke, M. E., Axelrad, P., Gold, K. L., Johnson, J., Key, K. W., Kubitschek, D. G. and Christensen, E. J. (1994). Calibration of the TOPEX altimeter using a GPS buoy. *Journal of Geophysical Research: Oceans.* 99 (C12), 24517-26.

Bouffard, J., Pascual, A., Ruiz, S., Faugère, Y. and Tintoré, J. (2010). Coastal and Mesoscale Dynamics Characterization using Altimetry and Gliders: A Case Study in the Balearic Sea. *Journal of Geophysical Research: Oceans.* 115 (C10), 1-17.

Bouffard, J., Vignudelli, S., Cipollini, P. and Menard, Y. (2008). Exploiting the Potential of an Improved Multimission Altimetric Data Set over the Coastal Ocean. *Geophysical Research Letters.* 35 (10), 1-6.

Briais, A., Patriat, P. and Tapponnier, P. (1993). Updated Interpretation of Magnetic Anomalies and Seafloor Spreading Stages in the South China Sea: Implications for the Tertiary Tectonics of Southeast Asia. *Journal of Geophysical Research: Solid Earth.* 98 (B4), 6299-328.

Bron, E., Guillot, A. and Picot, N. (2016). SARAL/AltiKa Product Handbook. *No. CNES: SALP-MU-M-OP-15984-CN.* 1-76.

Bronner, E. and Dibarboure, G. (2012). *Technical Note about the Jason-1 Geodetic Mission* Centre National d'Etudes Spatiales and National Aeronautics and Space Administration.

Brooks, R. L., Lockwood, D. W., Lee, J. E., Handcock, D. and Hayne, G. S. (1998). Land Effects on TOPEX Radar Altimeter Measurements on Pacific Rim Coastal Zones. *Remote Sensing of the Pacific by Satellites.* 175-98.

Brown, G. S. (1977). The Average Impulse Response of a Rough Surface and its Applications. *IEEE J. Oceanic Eng.* 2 67 - 74.

Brown, R. M., Siler, C. D., Oliveros, C. H., Esselstyn, J. A., Diesmos, A. C., Hosner, P. A., Linkem, C. W., Barley, A. J., Oaks, J. R. and Sanguila, M. B. (2013). Evolutionary Processes of Diversification in a Model Island Archipelago. *Annual Review of Ecology, Evolution, and Systematics.* 44 411-35.

Burton, T., Jenkins, N., Sharpe, D. and Bossanyi, E. (2011). *Wind Energy Handbook.* United Kingdom: John Wiley & Sons.

Cancet, M., Lux, M., Pénard, C., Lyard, F., Birol, F., Lemouroux, J., Bourgogne, S. and Bronner, E. (2010). COMAPI: New Regional Tide Atlases and High Frequency Dynamical Atmospheric Correction. *Ocean Surface Topography Science Team meeting.* 23 December. France,

Carrère, L. and Lyard, F. (2003). Modeling the Barotropic Response of The Global Ocean to Atmospheric Wind and Pressure Forcing-Comparisons with Observations. *Geophysical Research Letters.* 30 (6), 1275-8.

Carrère, L., Lyard, F., Cancet, M., Guillot, A. and Roblou, L. (2012). FES2012: A New Global Tidal Model Taking Advantage of Nearly 20 Years of Altimetry. *Progress in Radar Altimetry Symp.* Venice, Italy, 710.

Cartwright, D. and Edden, A. C. (1973). Corrected Tables of Tidal Harmonics. *Geophysical Journal International.* 33 (3), 253-64.

Cazenave, A., Dominth, F., Pochaut, F., Soudarin, L., Cretaux, J. F. and Le Provost, C. (1999). Sea Level Changes from Topex/Poseidon Altimetry and Tide Gauges, and Vertical Crustal Motion from Doris. *Geophysical Research Letters.* 26 (14), 2077-80.

Challenor, P. and Srokosz, M. (1989). The Extraction of Geophysical Parameters from Radar Altimeter Return from a Non-Linear Sea Surface. *Mathematics in remote sensing.* 257-68.

Challenor, P. G., Read, J. F., Pollard, R. T. and Tokmakin, R. T. (1996). Measuring Surface Current in Drake Passage fron Altimetry and Hydrography. *Journal of Physical Oceanography.* 26 (12), 2784 - 58.

Chang, C.-P. (2004). *East Asian Monsoon.* California, USA: World Scientific.

Chang, C.-P. and Chen, G. T.-J. (1995). Tropical Circulations Associated with Southwest Monsoon Onset and Westerly Surges over the South China Sea. *Monthly Weather Review.* 123 (11), 3254-67.

Chang, C.-P., T Angang, F., Aldrian, E., Koh, T. Y. and Juneng, L. (2004a). The Maritime Continent Monsoon. In Chang, C.-P. *East Asian Monsoon.* California, USA: World Scientific Publishing.

Chang, C.-P., Wang, Z., McBride, J. and Liu, C.-H. (2005). Annual Cycle of Southeast Asia - Maritime Continent Rainfall and the Asymmetric Monsoon Transition. *Journal of climate.* 18 (2), 287-301.

Chang, C., Wang, Z., Ju, J. and Li, T. (2004b). On the Relationship between Western Maritime Continent Monsoon Rainfall and ENSO During Northern Winter. *Journal of Climate.* 17 (3), 665-72.

Chang, R. (2013). The South China Sea. Terra Weather. Terra Weather.

Chaudhary, A., Agarwal, N. and Sharma, R. (2014). Estimation of Currents using SARAL/AltiKa in theCoastal Regions of India. *ISPRS - International Archives of the Photogrammetry, Remote Sensing and Spatial Information Sciences.* XL-8 1365-67.

Chen, G., Hou, Y. and Chu, X. (2011). Mesoscale eddies in the South China Sea: Mean Properties, Spatiotemporal Variability, and Impact on Thermohaline Structure. *Journal of Geophysical Research.* 116 (C6), 18-37.

Chen, M., Goodkin, N. F., Boyle, E. A., Switzer, A. D. and Bolton, A. (2016). Lead in the Western South China Sea: Evidence of Atmospheric Deposition and Upwelling. *Geophysical Research Letters.* 43 (9), 4490-99.

Chung, R. H., Zheng, Q., Soong, Y. S., Nan, J. K. and Jian, H. H. (2000). Seasonal Variability of Sea Surface Height in the South China Sea observed with TOPEX/Poseidon Altimeter Data. *Journal of Geophysical Research.* 105 13,981 - 13, 90.

Cipollini, P. (2013). The Coastal Zone: A Mission Target for Satellite Altimetry *Coastal Altimetry Workshop.* 7-8 October. Boulder, Colorado, 72.

Cipollini, P. (2015). *A Short Summary of the 9th Coastal Altimetry Workshop*: Series. A Short Summary of the 9th Coastal Altimetry Workshop, Workshop, C. A.

Cipollini, P., Benveniste, J., Bouffard, J., Emery, W. J., Fenoglio-Marc, L., Gommenginger, C., Griffin, D., Hoyer, J., Kurapov, A., Madsen, K., Mercier, F., Miller, L., Pascual, A., Ravichandran, M., Shillington, F., Snaith, H. M., Strub, P. T., Vandemark, D., Vignudelli, S., Wilkin, J., Woodworth, P. L. and Javier, Z. G. (2010). The Role of Altimetry in Coastal Observing Systems. *OceanObs.* 21 - 25 September. Venice, Italy,

Cipollini, P., Calafat, F. M., Jevrejeva, S., Melet, A. and Prandi, P. (2016). Monitoring Sea Level in the Coastal Zone with Satellite Altimetry and Tide Gauges. *Surveys in Geophysics.* 1-25.

Cipollini, P., Scarrott, R. and Snaith, H. (2013). *Product Data Handbook: Coastal Altimetry.* United Kingdom: European Space Agency

CNES (2010). Coastal and hydrology altimetry product (PISTACH) handbook. (1.0), 64.

Dac, D. N. (2013). *The Performance of SARAL/AltiKa in Coastal Region: Examples of the NW Mediterranean Sea and the South China Sea*. Master Degree. Toulouse, France.

Dangendorf, S., Wahl, T., Hein, H., Jensen, J., Mai, S. and Mudersbach, C. (2012). Mean Sea Level Variability and Influence of the North Atlantic Oscillation on Long-term Trends in the German Bight. *Water.* 4 (1), 170-95.

Davis, C. H. (1997). A Robust Threshold Retracking Algorithm for Measuring Ice-sheet Surface Elevation Change from Satellite Alimeters *IEEE Transaction on Geosciences and Remote Sensing.* 35 (4), 974 - 79.

Deng, X. and Featherstone, W. E. (2006). A coastal retracking system for satellite radar altimeter waveforms: Application to ERS-2 around Australia. *Journal of Geophysical Research.* 111 (C6), 12-28.

Deng, X., Featherstone, W. E., Hwang, C. and Berry, P. A. M. (2002). Estimation of Constamination of ERS-2 and POSEIDON Satellite Radar Altimetry Close to the Coasts of Australia. *Marine Geodesy.* 25 (4), 249-71.

Dettmering, D., Schwatke, C. and Bosch, W. (2014). Global Calibration of SARAL/AltiKa Using Multi-Mission Sea Surface Height Crossovers. *Marine Geodesy.* 38 (sup1), 206-18.

Din, A., Ses, S., Omar, K., Yaakob, O., Naeije, M. and Pa'suya, M. (2014). Derivation of sea level anomaly based on the best range and geophysical corrections for Malaysian seas using radar altimeter database system (RADS). *Jurnal Teknologi (Sciences And Engineering).* 71 (4), 83-91.

Dippner, J. W., Nguyen, K. V., Hein, H., Ohde, T. and Loick, N. (2007). Monsoon-induced Upwelling off the Vietnamese Coast. *Ocean Dynamics.* 57 (1), 46-62.

Ebdon, D. (1985). *Statistics in geography.*

Eshel, G. and Naik, N. H. (1997). Climatological Coastal Jet Collision, Intermediate Water Formation, and the General Circulation of The Red Sea. *Journal of Physical Oceanography.* 27 (7), 1233-57.

Fang, G., Wang, G., Fang, Y. and Fang, W. (2012). A review on the South China Sea western boundary current. *Acta Oceanologica Sinica.* 31 (5), 1-10.

Fang, G., Wang, Y., Wei, Z., Fang, Y., Qiao, F. and Hu, X. (2009). Interocean circulation and heat and freshwater budgets of the South China Sea based on a numerical model. *Dynamics of Atmospheres and Oceans.* 47 (1), 55-72.

Fernandes, J., Nunes, A. L., Lazaro, C., Pires, N., Bastos, L. and Mendes, V. B. (2008). Wet Trophospheric Correction for Coastal Altimetry Based on GNSS Path Delay Measurement. *Coastal Altimetry Workshop.* 6-7 November. Pisa, Italy,

Frappart, F., Papa, F., Marieu, V., Malbeteau, Y., Jordy, F., Calmant, S., Durand, F. and Bala, S. (2015). Preliminary Assessment of SARAL/AltiKa Observations over the Ganges-Brahmaputra and Irrawaddy Rivers. *Marine Geodesy.* 38 (sup1), 568-80.

Fu, L. L. and Cazenave, A. (2001). *Satellite Altimetry and Earth Sciences: A Handbook of Techniques and Applications* San Diego, California: Academic Press.

Fu, L. L., Christensen, E. J., Yamarone, C. A., Lefebvre, M., Menard, Y., Dorrer, M. and Escudier, P. (1994). TOPEX/POSEIDON Mission Overview. *Journal of Geophysical Research: Oceans.* 99 (C12), 24369-81.

Ganguly, D., Chander, S., Desai, S. and Chauhan, P. (2015). A Subwaveform-Based Retracker for Multipeak Waveforms: A Case Study over Ukai Dam/Reservoir. *Marine Geodesy.* 38 (sup1), 581-96.

Gill, A. and Niller, P. (1973). The Theory of the Seasonal Variability in the Ocean. *Deep Sea Research and Oceanographic Abstracts.* 20 (2), 141-77.

Gómez-Enri, J., Cipollini, P., Gommenginger, C., Martin-Puig, C., Vignudelli, S., Woodworth, P., Benveniste, J. and Villares, P. (2008). COASTALT: improving radar altimetry products in the oceanic coastal area. 7105 71050J1-10.

Gómez-Enri, J., Gommenginger, C. P., Srokosz, M. A., Challenor, P. G. and Benveniste, J. (2007a). Measuring Global Ocean Wave Skewness by Retracking RA-2 Envisat Waveforms. *Journal of Atmospheric and Oceanic Technology.* 24 (6), 1102-16.

Gómez-Enri, J., Villares, P., Gommenginger, C., Srokosz, M. A., Challenor, P., Alonso, J. J., Arias, M., Catalan Perez-Urquila, M. and Medina, C. (2007b). Retrieving the Ocean Wave-skewness from Envisat RA-2 Averanged Waveforms. *Envisat Symposium* 23 - 27 April.

Gommenginger, C., Thibaut, P., Fenodlio-Marc, L., Quartly, G., Deng, X., Gomez-Enri, J., Challenor, P. and Gao, Y. (2011). Retracking Altimeter Waveforms Near the Coasts. A Review of Retracking Methods and Some Applications to Coastal Waveforms. In Vignudelli, S., Kostianoy, A. G., P.Cipollini and Benveniste, J. *Coastal Altimetry.* (61-101). London, New York: Springer.

Gommenginger, C. P. and Srokosz, M. A. (2006). Sea State Bias–20 Years On. *SSB.* 1 (8), 1-.

Han, G. and Huang, W. (2009). Low-frequency sea-level variability in the South China Sea and its relationship to ENSO. *Theoretical and applied climatology.* 97 (1-2), 41-52.

Heliani, L. S., Widjajanti, N., Endrayanto, I. and Panuntun, H. (2013). Preprocessing of Coastal Satellite Altimetry, Tide Gauges, and GNSS Data: Towards the Possibility of Detected Vertical Deformation of South Java Island. *Procedia Environmental Sciences.* 17 308-16.

Ho, C.-R., Zheng, Q., Soong, Y. S., Kuo, N.-J. and Hu, J.-H. (2000). Seasonal variability of sea surface height in the South China Sea observed with TOPEX/Poseidon altimeter data. *Journal of Geophysical Research.* 105 (C6), 13981.

Hsu, S.-K., Yeh, Y.-c., Doo, W.-B. and Tsai, C.-H. (2004). New Bathymetry and Magnetic Lineations Identifications in The Northernmost South China Sea and Their Tectonic Implications. *Marine Geophysical Researches.* 25 (1-2), 29-44.

Hu, J. and Wang, X. H. (2016). Progress on Upwelling Studies in the China Seas. *Reviews of Geophysics.* 54 (3), 653-73.

Hwang, C. and Chen, S.-A. (2000). Circulations and Eddies over the South China Sea Derived from TOPEX/Poseidon Altimetry. *Journal of Geophysical Research.* 105 (C10), 23943.

Hwang, C., Guo, J., Deng, X., Hsu, H.-Y. and Liu, Y. (2006). Coastal Gravity Anomalies from Retracked Geosat/GM Altimetry: Improvement, Limitation and the Role of Airborne Gravity Data. *Journal of Geodesy.* 80 (4), 204-16.

Hyne, G. S. (1980). Radar Altimeter Mean Return Waveforms from Near-normal-incidence Ocean Surface Scattering. *IEEE Transaction on Antennas and Propagation.* 25 (5), 687 - 92.

Idris, N. H. (2014). *Development of New Retracking Methods for Mapping Sea Levels Over The Shelf Areas from Satellite Altimetry Data*. Doctor of Philosophy. Newcastle, Australia.

Idris, N. H., Abdullah, N. N., Idris, N. H. and Maharaj, A. (2016). Validation of Retracked Sea Levels for Saral/Altika Satellite Altimetry over the Continental Shelf of the South China Sea. *13th International Umt Annual Symposium UMTAS 2016.* 13-15 December. Malaysia, 222-30.

Idris, N. H. and Deng, X. (2013). An Iterative Coastal Altimetry Retracking Strategy Based on Fuzzy Expert System for Improving Sea Surface Height Estimates. *Geosciences and Remote Sensing Symposium (IGARSS).* 21-26 July. Melbourne, Australia, 2954-57.

Idris, N. H. and Deng, X. (2012). The Retracking Technique on Multi-Peak and Quasi-Specular Waveforms for Jason-1 and Jason-2 Missions near the Coast. *Marine Geodesy.* 35 (sup1), 217-37.

Idris, N. H., Deng, X. and Andersen, O. B. (2014a). The Importance of Coastal Altimetry Retracking and Detiding: A Case Study around the Great Barrier Reef, Australia. *International Journal of Remote Sensing.* 35 (5), 1729-40.

Idris, N. H., Deng, X. and Idris, N. H. (2017a). Comparison of retracked coastal altimetry sea levels against high frequency radar on the continental shelf of the Great Barrier Reef, Australia. *Journal of Applied Remote Sensing.* 11 (3), 032403-03.

Idris, N. H., Deng, X., Md Din, A. H. and Idris, N. H. (2017b). CAWRES: A Waveform Retracking Fuzzy Expert System for Optimizing Coastal Sea Levels from Jason-1 and Jason-2 Satellite Altimetry Data. *Remote Sensing.* 9 (6), 603.

Idris, N. H., Maharaj, A., Abdullah, N. N., Deng, X. and Andersen, O. B. (2014b). A Comparison of Saral/Altika Coastal Altimetry and In-Situ Observation Across Australasia and Maritime Continent. *SARAL/AltiKa Workshop.* 27-31 October 2014. Lake Constant, Germany,

Idris, N. H., Maharaj, A., Deng, X., Abdullah, N. N., Idris, N. H. and Wan Kadir, W. H. (2014c). A Comparison of Saral/Altika Coastal Altimetry and In-Situ Observation Across Australasia And Maritime Continent. *Australia Coastal Ocean Modelling and Observations.* 7-8 October 2014. Canberra, Australia,

Idris, N. H. and Mohd, M. I. S. (2007). Sea Surface Current Circulation Pattern in the South China Sea Derived from Satellite Altimetry. *Asian Conference on Remote Sensing.* 12-17 November. Kuala Lumpur,

Kämpf, J. and Chapman, P. (2016). The Functioning of Coastal Upwelling Systems. In *Upwelling Systems of the World.* (31-65). Springer.

Kok, P. H., Akhir, M. F. M., Tangang, F. and Husain, M. L. (2017). Spatiotemporal Trends in the Southwest Monsoon Wind-Driven Upwelling in the Southwestern Part of The South China Sea. *PloS One.* 12 (2), e0171979.

Kuo, C.-Y., Kao, H.-C., Lee, H., Cheng, K.-C. and Lin, L.-C. (2012). Assessment of Radar Waveform Retracked Jason-2 Altimetry Sea Surface Heights Near Taiwan Coastal Ocean. *Marine Geodesy.* 35 (2), 188-97.

Kuo, H. T., Shum, C. K., Chao, Y., Emery, W. J., Fok, H., Lee, H., Kuo, C.-Y. and Yi, Y. (2011). Radar Altimetry Waveform Retracking Applied to Coastal Ocean. *5th Coastal Altimetry Workshop.* 16-18 October.

Kuo, N.-J., Zheng, Q. and Ho, C.-R. (2004). Response of Vietnam Coastal Upwelling to the 1997–1998 ENSO Event Observed by Multisensor Data. *Remote sensing of environment.* 89 (1), 106-15.

Kuo, N.-J., Zheng, Q. and Ho, C.-R. (2000). Satellite Observation of Upwelling along the Western Coast of the South China Sea. *Remote Sensing of Environment.* 74 (3), 463-70.

Le Traon, P.-Y. (2011). Satellites and operational oceanography. In *Operational Oceanography in the 21st Century.* (29-54). Springer.

Le Traon, P.-Y., Antoine, D., Bentamy, A., Bonekamp, H., Breivik, L., Chapron, B., Corlett, G., Dibarboure, G., DiGiacomo, P. and Donlon, C. (2015). Use of satellite observations for operational oceanography: recent achievements and future prospects. *Journal of Operational Oceanography.* 8 (sup1), s12-s27.

Le Traon, P. Y. and Morrow, R. (2001). Ocean Currents and Eddies. In Fu, L. L. and Cazenave, A. *Satellite Altimetry and Earth Sciences: a Handbook of Techniques and Applications.* (171-217). Sydney, Australia: Academic Press.

Lebedev, S., Sirota, A., Medvedev, D., Khlebnikova, S., Vignudelli, S., Snaith, H. M., Cipollini, P., Venuti, F., Lyard, F., Bouffard, J., Cretaux, J. F., Birol, F., Roblou, L., Kostianoy, A. G., Ginzburg, A., Sheremet, N., Kuzminz, E., R., M., Ismatova, K., Alyev, A. and Mustafayev, B. (2008). Exploiting Satellite Altimetry in Coastal Ocean Through the ALTICORE Project. *Russian Journal of Earth Sciences.* 10 (ES1002), 1-11.

Lee, H., Shum, C. K., Emery, W., Calmant, S., Deng, X., Kuo, C.-Y., Roesler, C. and Yi, Y. (2010). Validation of Jason-2 Altimeter Data by Waveform Retracking over California Coastal Ocean. *Marine Geodesy.* 33 (sup1), 304-16.

Legresy, B., Papa, F., Remy, F., Vinay, G., Van Den Bosch, M. and Zanife, O.-Z. (2005). ENVISAT Radar Altimeter Measurements over Continental Surfaces and Ice Caps using the ICE-2 Retracking Algorithm. *Remote Sensing of Environment.* 95 (2), 150-63.

Liebsch, G., Novotny, K., Dietrich, R. and Shum, C. K. (2002). Comparison of Multimission Altimetric Sea-Surface Heights with Tide Gauge Observations in the Southern Baltic Sea. *Marine Geodesy.* 25 (3), 213-34.

Lin, N., Smith, J. A., Villarini, G., Marchok, T. P. and Baeck, M. L. (2010). Modeling Extreme Rainfall, Winds, and Surge from Hurricane Isabel (2003). *Weather and Forecasting.* 25 (5), 1342-61.

Liu, Q. (2004). A gap in the Indo-Pacific warm pool over the South China Sea in boreal winter: Seasonal development and interannual variability. *Journal of Geophysical Research.* 109 (C7),

Liu, Z., Yang, H. and Liu, Q. (2001). Regional dynamics of seasonal variability in the South China Sea. *Journal of physical oceanography.* 31 (1), 272-84.

Lyard, F., Fabien, L., Letellier, T. and Francis, O. (2006). Modelling the Global Ocean Tides: Modern Insights from FES2004. *Ocean Dynamics.* 56 (5-6), 394 - 415.

Mansor, K. N. A. A. K., Pa'suya, M. F., Abbas, M. A., Ali, T. A. T., Aziz, M. A. C. and Md Din, A. H. (2016). Ocean Surface Circulation in Strait of Malacca using Satellite Altimeter and Low Cost GPS-tracked Drifting BSuoys. *Control and System Graduate Research Colloquium (ICSGRC), 2016 7th IEEE.* 175-80.

Manzella, G. M. R., Borzelli, G. L., Cipollini, P., Guymer, T. H., Snaith, H. M. and Vignudelli, S. (1997). Potential Use of Satellite Data to Infer the Circulation Dynamics in a Marginal Area of the Mediterranean Sea. *3rd ERS Symposium - Space at Service of our Envirenment.* 17-21 March. Florence, Italy,

McCarthy, G. D., Haigh, I. D., Hirschi, J. J.-M., Grist, J. P. and Smeed, D. A. (2015). Ocean Impact on Decadal Atlantic Climate Variability Revealed by Sea-Level Observations. *Nature.* 521 (7553), 508-10.

Md Din, A. H. (2014). *Sea Level Rise Estimation and Interpretation in Malaysian Region Using Multi-sensor Techniques*. Doctor of Philosophy. Johor, Malaysia.

Md Din, A. H. (2010). *Sea Level Rise Estimation Using Satellite Altimetry Technique*. Master Degree. Johor, Malaysia.

Md Din, A. H. and Omar, K. M. (2009). Sea level change in the Malaysian seas from multi-satellite altimeter data.

Md Din, A. H. and Omar, K. M. (2012). Sea Level Change in the Malaysian Seas from Multi-Satellite Altimeter Data.

Md Din, A. H., Omar, K. M., Naeije, M. C. and Ses, S. (2012). Long-term sea level change in the Malaysian seas from multi-mission altimetry data. *International Journal of the Physical Sciences.* 7 (10), 1694-712.

Melsheimer, C. and Chin, L. S. (2001). Extracting Bathymetry from Multi-temporal SPOT Images. *Paper presented at the 22nd Asian Conference on Remote Sensing.* 9.

Menendez, M., Mendez, F. J. and Losada, I. J. (2009). Forecasting seasonal to interannual variability in extreme sea levels. *ICES Journal of Marine Science.* 66 (7), 1490-96.

Mohammed, S. B., Idris, N. H. and Abdullah, N. N. (2015). Along-Track High Resolution Sea Levels from SARAL/Altika Satellite Altimetry Data over The Maritime Continent *IEEE Workshop on Geoscience and Remote Sensing.* 16-17 November. Kuala Lumpur, Malaysia, 90-93.

Mohd Akhir, M. and Chuen, Y. (2011). Seasonal Variation of Water Characteristics during Inter-monsoon aong the East Coast of Johor. *Journal of Sustainability Science and Management.* 6 (2), 206-14.

Mohd Akhir, M. F. (2012). Surface Circulation and Temperature Distribution of Sothern South China Sea from Global Ocean Model (OCCAM). *Sains Malaysiana.* 41 (6), 701-14.

Mohd Akhir, M. F., Daryabor, F., Husain, M. L., Tangang, F. and Qiao, F. (2015). Evidence of Upwelling Along Peninsular Malaysia during Southwest Monsoon. *Open Journal of Marine Science.* 5 (03), 273.

Mohd Akhir, M. F., Zakaria, N. Z. and Tangang, F. (2014). Intermonsoon Variation of Physical Characteristics and Current Circulation along the East Coast of Peninsular Malaysia. *International Journal of Oceanography.* 2014 1-9.

Nayak, R., Salim, M., Sasamal, S., Mohanthy, P., Bharadwaj, R., Rao, K., Dutt, C. and Dadhwal, V. (2016). Assessment of SARAL-ALTIKA Tidal Corrections in the Coastal Oceans Around India. *Marine Geodesy.* 39 (5), 331-47.

Nerem, R. and Mitchum, G. (2002). Estimates of vertical crustal motion derived from differences of TOPEX/POSEIDON and tide gauge sea level measurements. *Geophysical Research Letters.* 29 (19),

Neumann, B., Vafeidis, A. T., Zimmermann, J. and Nicholls, R. J. (2015). Future Coastal Population Growth and Exposure to Sea-Level Rise and Coastal Flooding-A Global Assessment. *PloS One.* 10 (3), e0118571.

Obligis, E., Desportes, C., Eymard, L., Fernandes, J., Lazaro, C. and Nunes, A. L. (2011). Tropospheric Corrections for Coastal Altimetry In Valladeau, G., Kostianoy, A. G., Cipollini, P. and Benveniste, J. *Coastal Altimetry.* (147 - 76). Berlin: Springer.

Obligis, E., Mercier, F., Picard, B. and Desportes, C. (2008). Land Decontamination Method for Wet Trophospheric Correction Retrieval. *Coastal Altimetry Workshop.* 6 -7 November. Pisa, Italy,

Pa'suya, M. F., Omar, K. M., Peter, B. N., Md Din, A. H. and Akhir, M. F. M. (2014). Seasonal Variation of Surface Circulation Along Peninsular Malaysia'East Coast. *Jurnal Teknologi.* 71 (4),

Palanisamy, H., Cazenave, A., Henry, O., Prandi, P. and Meyssignac, B. (2015). Sea-Level Variations Measured by the New Altimetry Mission SARAL/AltiKa and its Validation Based on Spatial Patterns and Temporal Curves Using Jason-2, Tide Gauge Data and an Overview of the Annual Sea Level Budget. *Marine Geodesy.* 38 (sup1), 339-53.

Pascual, A., Lana, A., Troupin, C., Ruiz, S., Faugère, Y., Escudier, R. and Tintoré, J. (2015). Assessing SARAL/AltiKa data in the coastal zone: comparisons with HF radar observations. *Marine Geodesy.* 38 (sup1), 260-76.

Passaro, M., Cipollini, S., Vignudelli, G. Q. and Snaith, H. M. (2014). ALES: A Multi-mission Adaptive Subwaveform Retracker for Coastal and Open Ocean Altimetry. *Remote Sensing Environment.* 145 173-89.

Pattiaratchi, C. and Wijeratne, E. (2014). Observations of Meteorological Tsunamis along the South-West Australian Coast. *Natural hazards.* 74 (1), 281-303.

Pattullo, J., Munk, W., Revelle, R. and Strong, E. (1955). The Seasonal Oscillation in Sea Level. *J. mar. Res.* 14 (1), 88-156.

Pavlis, N. K. and Holmes, S. A. (2004). A preliminary gravitational model to degree 2160. *IAG International Symposium on Gravity, Geoid and Space Missions 2004.* 30 August- 3 September. Porto, Portugal,

Pavlis, N. K., Holmes, S. A., Kenyon, S. C. and Factor, J. K. (2012). The development and evaluation of the Earth Gravitational Model 2008 (EGM2008). *Journal of Geophysical Research: Solid Earth.* 117 (B4), 4406-44.

Pawlowicz, R., Beardsley, B. and Lentz, S. (2002). Classical tidal harmonic analysis including error estimates in MATLAB using T_TIDE. *Computers & Geosciences.* 28 (8), 929-37.

Poisson, J. C., Thibaut, P. and Valladeau, G. (2013). Processing of Altika Waveform: New Retracking Algorithms Implemented in the PEACHI Project. *AltiKa CalVal Meeting.* 27 March. Toulouse, France,

Prandi, P., Philipps, S., Pignot, V. and Picot, N. (2015). SARAL/AltiKa Global Statistical Assessment and Cross-Calibration with Jason-2. *Marine Geodesy.* 38 (sup1), 297-312.

Qu, T., Song, Y. T. and Yamagata, T. (2009). An introduction to the South China Sea throughflow: Its dynamics, variability, and application for climate. *Dynamics of Atmospheres and Oceans.* 47 (1), 3-14.

Ratheesh, S., Sharma, R., Prasad, K. V. S. R. and Basu, S. (2015). Impact of SARAL/AltiKa-Derived Sea Level Anomaly in a Data Assimilative Ocean Prediction System for the Indian Ocean. *Marine Geodesy.* 38 (sup1), 354-64.

Ray, R. (2008). Tide Corrections for Shallow-Water Altimetry. *Coastal Altimetry Workshop.* 6 - 7 November. Pisa, Italy,

Rémy, F., Flament, T., Michel, A. and Blumstein, D. (2014). Envisat and SARAL/AltiKa Observations of the Antarctic Ice Sheet: A Comparison Between the Ku-band and Ka-band. *Marine Geodesy.* 38 (sup1), 510-21.

Robertson, A. W., Moron, V., Qian, J., Chang, C., Tangang, F., Aldrian, E., Koh, T. Y. and Juneng, L. (2011). The Maritime Continent Monsoon. *The Global Monsoon System: Research and Forecast.* 85-98.

Rodriguez, E. (1988). Altimetry for Non-Gaussian Oceans: Height Biases and Estimation of Parameters. *Journal Geophysical Research* 93 (C11), 14107-20.

Roesler, C. J., Emery, W. J. and Kim, S. Y. (2013). Evaluating the Use of High-frequency Radar Coastal Currents to Correct Satellite Altimetry. *Journal of Geophysical Research.* 118 3240 - 59.

Rosmorduc, V., Benveniste, J., Lauret, O., Maheu, C., Milagro, M. and Picot, N. (2011). Radar Altimetry Tutorial. *ESA, Europe.* 112-28.

Roughan, M., Keating, S., Schaeffer, A., Cetina Heredia, P., Rocha, C., Griffin, D., Robertson, R. and Suthers, I. (2017). A Tale of Two Eddies: The Biophysical Characteristics of Two Contrasting Cyclonic Eddies in the East Australian Current System. *Journal of Geophysical Research: Oceans.* 122 (3), 2494-518.

Saha, K. (2010). Meteorology of the Maritime Continent (Region – III) (Comprising Philippines, Indonesia and Equatorial Western Pacific Ocean). In *Tropical Circulation Systems and Monsoons.* (155-69). Berlin Heidelberg: Springer.

Salahuddin, A. and Curtis, S. (2011). Climate Extremes in Malaysia and the Equatorial South China Sea. *Global and Planetary Change.* 78 (3), 83-91.

Saramul, S. and Ezer, T. (2014). Spatial variations of sea level along the coast of Thailand: impacts of extreme land subsidence, earthquakes and the seasonal monsoon. *Global and Planetary Change.* 122 70-81.

Satellites, C. L. (2011). Validation of Altimetric Data by Comparison with Tide Gauge Measurements for TOPEX/Poseidon, Jason-1, Jason-2 and Envisat. Annual report Insitu. 1 (1), 10 - 289.

Schureman, P. (1958). *Manual of harmonic analysis and prediction of tides.* US Government Printing Office.

Schureman, P. (1976). *Manual of harmonic analysis and prediction of tides.* US Department of Commerce, Coast and Geodetic Survey.

Schwatke, C., Dettmering, D., Börgens, E. and Bosch, W. (2015). Potential of SARAL/AltiKa for Inland Water Applications. *Marine Geodesy.* 38 (sup1), 626-43.

Shaw, P.-T., Chao, S.-Y. and Fu, L.-L. (1999). Sea Surface Height Variations in the South China Sea from Satellite Altimetry. *Oceanologica Acta.* 22 (1), 1-17.

Silver, W. and Buckley, J. J. (2005). *Fuzzy Expert Systems and Fuzzy Reasoning.* USA: Wiley.

Strachan, J. and Vidale, P. L. (2013). Investigating Global Tropical Cyclone Activity with a Hierarchy of AGCMs: The Role of Model Resolution. *Journal of Climate.* 26 (1), 133-52.

Strub, T. (2001). High-Resolution Ocean Topography Science Requirements for Coastal Studies. *Report of the High-Resolution Ocean Topography Science Working Group Meeting.* 4 October. United States, 33.

Sudre, J., Maes, C. and Garçon, V. (2013). On the global estimates of geostrophic and Ekman surface currents. *Limnology and Oceanography: Fluids and Environments.* 3 (1), 1-20.

Thibaut, P., Poisson, J. C., Bronner, E. and Picot, N. (2010). Relative Performance of the MLE3 and MLE4 Retracking Algorithms on Jason-2 Altimeter Waveforms. *Marine Geodesy.* 33 (S1), 317 - 35.

Tkalich, P., Vethamony, P., Luu, Q.-H. and Babu, M. (2013). Sea Level Trend and Variability in the Singapore Strait. *Ocean Science.* 9 (2013), 293-300.

Tokeshi, R., Ichikawa, K., Fujii, S., Sato, K. and Kojima, S. (2007). Estimating the Geostrophic Velocity Obtained by HF Radar Observations in the Upstream Area of the Kuroshio. *Journal of Oceanography.* 63 (4), 711-20.

Tournadre, J. (1999). Estimation of Rainfall from Ka-band Altimetry Data: Computation of Waveform in Presence of Variable Cloud and Rain Attenuation. *IGARSS.* Jun. 28 - Jul. 2. Hamburg, Germany, 197-99.

Tournadre, J., Lambin, J. and Steunou, N. (2009). Cloud and Rain Effect on AltiKa/SARAL Ka-band Radar Altimeter - Part I: Modelling and Mean Annual Data Availability *IEEE Transactions on Geoscience and Remote Sensing.* 47 (6), 1806-17.

Tournadre, J., Poisson, J., Steunou, N. and Picard, B. (2015). Validation of AltiKa matching pursuit rain flag. *Marine Geodesy.* 38 (sup1), 107-23.

Trisirisatayawong, I., Naeije, M., Simons, W. and Fenoglio-Marc, L. (2011). Sea Level Change in the Gulf of Thailand from GPS-corrected tide Gauge Data and Multi-Satellite Altimetry. *Global and Planetary Change.* 76 (3), 137-51.

Tseng, K.-H., Shum, C., Yi, Y., Emery, W. J., Kuo, C.-Y., Lee, H. and Wang, H. (2014). The Improved Retrieval of Coastal Sea Surface Heights by Retracking Modified Radar Altimetry Waveforms. *IEEE Transactions on Geoscience and Remote Sensing.* 52 (2), 991-1001.

Tsimplis, M. and Woodworth, P. (1994). The global distribution of the seasonal sea level cycle calculated from coastal tide gauge data. *Journal of Geophysical Research: Oceans.* 99 (C8), 16031-39.

Ulaby, F. T., Moore, R. K. and Fung, A. K. (1981). *Microwave Remote Sensing: Radar Remote Sensing and Surface Scattering and Emission Theory.* Addison-Wesley, Advance Science Program/World Science Division.

Valladeau, G., Legeais, J. F., Ablain, M., Guinehut, S. and Picot, N. (2012). Comparing Altimetry with Tide Gauges and Argo Profiling Floats for Data Quality Assessment and Mean Sea Level Studies. *Marine Geodesy.* 35 (sup1), 42-60.

Valladeau, G., Thibaut, P., Guillot, A. and Picot, N. (2014). On the Use of the PEACHI Prototype to Improve Ka-band Altimeter Data Along Coastal Areas. *Coastal Altimetry Workshop.* Lake Constance, Germany,

Valladeau, G., Thibaut, P., Picard, B., Poisson, J. C., Tran, N., Picot, N. and Guillot, A. (2015). Using SARAL/AltiKa to Improve Ka-band Altimeter Measurements for Coastal Zones, Hydrology and Ice. The PEACHI Prototype. *Marine Geodesy.* 38 (sup1), 124-42.

Varikoden, H., Preethi, B., Samah, A. and Babu, C. (2011). Seasonal Variation of Rainfall Characteristics in Different Intensity Classes over Peninsular Malaysia. *Journal of hydrology.* 404 (1), 99-108.

Vermeer, M., Kakkuri, J., Mälkki, P., Boman, H., Kahma, K. K. and Leppäranta, M. (1988). Land uplift and sea level variability spectrum using fully measured monthly means of tide gauge readings.

Verron, J., Sengenes, P., Lambin, J., Noubel, J., Steunou, N., Guillot, A., Picot, N., Coutin-Faye, S., Sharma, R., Gairola, R. M., Murthy, D. V. A. R., Richman, J. G., Griffin, D., Pascual, A., Remy, F. and Gupta, P. K. (2015). The SARAL/AltiKa Altimetry Satellite Mission. *Marine Geodesy.* 38 (sup1), 2-21.

Vignudelli, S., Cipollini, P., Roblou, L., Lyard, F., Gasparini, G. P., Manzella, G. and Astraldi, M. (2005). Improved Satellite Altimetry in Coastal Systems: Case Study of the Corsica Channel (Maditerranean Sea). *Geophysical Research Letters.* 32 7608-13.

Vignudelli, S., Kostianoy, A. G., Cipollini, P. and Benveniste, J. (2011). *Coastal Altimetry.* Berlin: Springer.

Vincent, P., Steunou, N., Caubet, E., Phalippou, L., Rey, L., Thouvenot, E. and Verron, J. (2006). AltiKa: A Ka-band Altimetry Payload and System for Operational Altimetry during the GMES Period. *Sensors.* 6 (3), 208-34.

Voris, H. K. (2000). Maps of Pleistocene Sea Levels in Southeast Asia: Shorelines, River Systems and Time Durations. *Journal of Biogeography.* 27 (5), 1153-67.

Wahl, T., Calafat, F. M. and Luther, M. E. (2014). Rapid changes in the seasonal sea level cycle along the US Gulf coast from the late 20th century. *Geophysical Research Letters.* 41 (2), 491-98.

Wang, D.-P., Flagg, C. N., Donohue, K. and Rossby, H. T. (2010). Wavenumber Spectrum in the Gulf Stream from Shipboard ADCP Observations and Comparison with Altimetry Measurements. *Journal of Physical Oceanography.* 40 (4), 840-44.

Wang, L., Sarnthein, M., Erlenkeuser, H., Grimalt, J., Grootes, P., Heilig, S., Ivanova, E., Kienast, M., Pelejero, C. and Pflaumann, U. (1999). East Asian Monsoon Climate during the Late Pleistocene: High-Resolution Sediment Records from the South China Sea. *Marine Geology.* 156 (1), 245-84.

Wang, P. and Li, Q. (2009). Oceanographical and Geological Background. *The South China Sea.* 25-73.

Watson, C., Coleman, R., White, N., Church, J. and Govind, R. (2003). Absolute calibration of TOPEX/Poseidon and Jason-1 using GPS buoys in bass strait, Australia special issue: Jason-1 calibration/validation. *Marine Geodesy.* 26 (3-4), 285-304.

Watson, C., White, N., Coleman, R., Church, J., Morgan, P. and Govind, R. (2004). TOPEX/Poseidon and Jason-1: Absolute calibration in Bass Strait, Australia. *Marine Geodesy.* 27 (1-2), 107-31.

Watson, C. S. (2005). *Satellite altimeter calibration and validation using GPS buoy technology*.

Wentz, F. J. (1992). Measurement of Oceanic Wind Vector using Satellite Microwave Radiometers. *IEEE Transactions on Geoscience and Remote Sensing.* 30 (5), 960-72.

Wingham, D., Francis, C., Baker, S., Bouzinac, C., Brockley, D., Cullen, R., de Chateau-Thierry, P., Laxon, S., Mallow, U. and Mavrocordatos, C. (2006). CryoSat: A Mission to Determine the Fluctuations in Earth's Land and Marine Ice Fields. *Advances in Space Research.* 37 (4), 841-71.

Wingham, D. J., Rapley, C. G. and Griffiths, H. (1986). New Techniques in Satellite Tracking Systems. In IGARSS. *86 Symposium Digest* September. Zurich, Switzerland, 185-90.

Wunsch, C. and Stammer, D. (1997). Atmospheric Loading and the Oceanic "Inverted Barometer" Effect. *Reviews of Geophysics.* 35 (1), 79-107.

Wyrtki, K. (1961). Physical Oceanography of the Southeast Asian Waters. *Scripps Institution of Oceanography.* 195 (2),

Xu, X.-z. (1982). The General Descriptions of the Horizontal Circulation in the South China Sea. *Proceedings of the 1980 of the Chinese Society of Marine Hydrology and Meteorology.* China,

Xu, Y.-L. (2013). *Wind effects on cable-supported bridges.* John Wiley & Sons.

Yang, L., Lin, M., Liu, Q. and Pan, D. (2012). A coastal altimetry retracking strategy based on waveform classification and sub-waveform extraction. *International Journal of Remote Sensing.* 33 (24), 7806-19.

Yi, J., Du, Y., He, Z. and Zhou, C. (2014). Enhancing the Accuracy of Automatic Eddy Detection and the Capability of Recognizing the Multi-Core Structures from Maps of Sea Level Anomaly. *Ocean Science.* 10 (1), 39-48.

Zainol, Z. and Mohd Akhir, M. F. (2016). Coastal Upwelling at Terengganu and Pahang Coastal Waters: Interaction of Hydrography, Current Circulation and Phytoplankton Biomass. *Jurnal Teknologi.* 78 (8), 11-27.

Zhang, B., Cao, C., Lillibridge, J. and Miller, L. (2015). Assessing the Measurement Consistency Between the Jason-2/AMR and SARAL/AltiKa/DFMR Microwave Radiometers Using Simultaneous Nadir Observations. *Marine Geodesy.* 38 (sup1), 143-55.

Zhang, T., Yang, S., Jiang, X. and Zhao, P. (2016). Seasonal–Interannual Variation and Prediction of Wet and Dry Season Rainfall over the Maritime Continent:

Roles of ENSO and Monsoon Circulation. *Journal of Climate.* 29 (10), 3675-95.

Zhang, Z., Chan, J. C. and Ding, Y. (2004). Characteristics, Evolution and Mechanisms of the Summer Monsoon Onset over Southeast Asia. *International Journal of Climatology.* 24 (12), 1461-82.

Zheng, F., Westra, S. and Sisson, S. A. (2013). Quantifying the dependence between extreme rainfall and storm surge in the coastal zone. *Journal of Hydrology.* 505 172-87.

Zheng, Z.-W., Zheng, Q., Kuo, Y.-C., Gopalakrishnan, G., Lee, C.-Y., Ho, C.-R., Kuo, N.-J. and Huang, S.-J. (2016). Impacts of Coastal Upwelling off East Vietnam on the Regional Winds System: An Air-sea-land Interaction. *Dynamics of Atmospheres and Oceans.* 76 105-15.

Zhou, J., Li, P. and Yu, H. (2012). Characteristics and mechanisms of sea surface height in the South China Sea. *Global and Planetary Change.* 88 20-31.

Zhuang, W., Qiu, B. and Du, Y. (2013). Low-frequency western Pacific Ocean sea level and circulation changes due to the connectivity of the Philippine Archipelago. *Journal of Geophysical Research: Oceans.* 118 (12), 6759-73.

Zhuang, W., Xie, S. P., Wang, D., Taguchi, B., Aiki, H. and Sasaki, H. (2010). Intraseasonal Variability in Sea Surface Height over the South China Sea. *Journal of Geophysical Research: Oceans.* 115 (C4),